

THE PROJECT REPORT ON
“MODELLING AND SIMULATION OF BIPEDAL ROBOT”



**U.V. Patel
College of
Engineering**

**THE PROJECT REPORT SUBMITTED IN
PARTIAL FULFILLMENT OF THE REQUIREMENT FOR
THE DEGREE OF MECHANICAL ENGINEERING**

**SUBMITTED BY
SUBHASHIS HANSDA (17012031044)**

**UNDER THE GUIDANCE OF
PROF. TRUSHAR R. SHAH
ASSISTANT PROFESSOR
DEPARTMENT OF MECHATRONICS ENGINEERING**

**AT
DEPARTMENT OF MECHANICAL ENGINEERING
U.V. PATEL COLLEGE OF ENGINEERING
GANPAT UNIVERSITY – 384012**



॥ विद्या समाजोत्कर्षः ॥

U.V. Patel
College of
Engineering

CERTIFICATE

This is to certify that the project entitled “Modelling and Simulation of Bipedal Robot” has been carried out by following group of students of class VIIIth Mechanical Engineering, Mechanical Engineering Department of U.V. Patel College of Engineering, under the guidance of Prof. Trushar R. Shah, Assistant Professor, Department of Mechatronics Engineering, towards the partial fulfillment of the requirements for the Degree of Bachelor of Technology in Mechanical Engineering of Ganpat University, Kherva

(1) Subhashis Hansda (17012031044)

(2) Kunjal Patel (17012031025)

(3) Sachin Panchal (17012031021)

DATE: 26/04/2020

PLACE: Ganpat University, Kherva

SIGNATURE OF GUIDE:

SIGNATURE OF INTERNAL EXAMINER:

SIGNATURE OF EXTERNAL EXAMINER:

SIGNATURE OF HEAD OF DEPARTMENT:

ACKNOWLEDGEMENT

It is my deepest sense of gratitude to my mentor and guide at college Prof. Trushar R. Shah (Assistant Professor), Department of Mechatronics Engineering, U.V. Patel College of Engineering for careful and precious guidance, which were extremely valuable for my study, both theoretically and practically.

I perceive as this opportunity as a big milestone in my career development. I will strive to use gained skills and knowledge in the best possible ways and I will continue to work on their improvement in order to attain desired career objectives.

Sincerely,
Subhashis Hansda
Kunjali Patel
Sachin Panchal

ABSTRACT

Biped robots have better mobility than conventional wheeled robots, but they tend to tip over easily. To be able to walk stably in various environments, such as on rough terrain, up and down slopes, or in regions containing obstacles, it is necessary for the robot to adapt to the ground conditions with a foot motion, and maintain its stability with a torso motion. When the ground conditions and stability constraint are satisfied, it is desirable to select a walking pattern that requires small torque and velocity of the joint actuators.

We first formulate the constraints of the foot motion parameters. By varying the values of the constraint parameters, we can produce different types of foot motion to adapt to ground conditions. We then propose a method for formulating the problem of the smooth hip motion with the largest stability margin, and derive the trajectory by iterative computation.

Finally, the correlation between the actuator specifications and the walking patterns is described through simulation studies, and the effectiveness of the proposed methods is confirmed by simulation examples and analysis report of the designed parts and assemblies.

INDEX

Sr. No.	Content	Page No.
	Acknowledgement	i.
	Abstract	ii.
	Index	iii.
	List of figure	iv.
	List of table	v.
1	Introduction	1
1.1	Background	1
1.2	The walking robotics control problem	1
1.3	The machine learning hypothesis	1
1.4	Objective	2
1.5	Why humanoid robot	2
2	Mechanism of humanoid robot	3
2.1	Design of mechanism of leg movement	3
2.2	Design of mechanism of arm articulation	4
3	Hardware of humanoid robot	5
3.1	Actuators	5
3.2	Accelerator and gyroscopes	5
3.3	Force sensing resistor	5
3.4	CMOS sensor	6
3.5	External circuits	6
3.6	Processor	6
4	Modelling and reference trajectory planning	7
4.1	Forward kinematics	7
4.2	Inverse kinematics	8
4.3	Zero moment point	9
4.4	Linear inverted pendulum model	10
4.5	Table cart model	11
4.7	Fourier approximation of CoM trajectories	11
4.8	Swing foot reference trajectories	12
5	Design of parts and assemblies	13
5.1	Actuator base	13
5.2	Actuator joint top	13
5.3	Actuator joint bottom	14
5.4	Actuator assembly	14
5.5	Hand upper arm	15
5.6	Hand lower arm	15
5.7	Hand assembly	16
5.8	Leg upper	16

5.9	Leg lower	17
5.10	Leg assembly	17
5.11	Chest upper body	18
5.12	Chest lower body	18
5.13	Chest upper link	19
5.14	Chest lower link	19
5.15	Chest assembly	20
6	Adaptive CMAC based dynamic balancing and ZMP compensation design	21
6.1	CMAC	21
6.2	RCMAC	21
6.3	Adaptive CMAC control system	21
6.4	ACMAC based dynamic balancing	22
6.5	ACMAC based ZMP compensator	22
6.6	Online learning algorithm	22
7	Mechanics of robot	23
7.1	Mechanism	23
7.2	Leg mechanism	23
8	LIPM	24
8.1	Assumptions	24
8.2	Finding initial conditions	24
8.3	Setting parameters	25
8.4	Finding joint angles	25
9	Simulation	27
10	Graphs	28
11	Conclusion	31
11.1	Conclusion based on theory and calculations	31
11.2	Conclusion based on analysis report	31
11.3	Extensions of work	31
12	Bibliography	32

LIST OF FIGURES

Fig. No.	Title	Page No.
1	Different link length will cause displacement of CoG	3
2	Different leg length will cause large displacement	3
3	Arm joint angles	4
4	Arm joint geometric representation	4
5	BLDC motor	5
6	ADXRS300	5
7	CMOS sensor	6
8	Rasberry pi 3B+	6
9	Position sense of twist angle	7
10	Zero moment point	9
11	Actual ZMP	10
12	LIPM	10
13	Table cart model	11
14	Swing foot reference trajectories	12
15	Design of actuator base	13
16	Design of actuator joint top	13
17	Design of actuator joint bottom	14
18	Design of actuator assembly	14
19	Design of hand upper arm	15
20	Design of hand lower arm	15
21	Design of hand assembly	16
22	Design of leg upper	16
23	Design of leg lower	17
24	Design of leg assembly	17
25	Design of chest upper body	18
26	Design of chest lower body	18
27	Design of chest upper link	19
28	Design of chest lower link	19
29	Design of chest assembly	20
31	Mechanism of robot	23
32	Leg mechanism of robot	23
33	LIPM symmetry 1	24
34	LIPM symmetry 2	24
35	CoM trajectory	25
36	DH parameters	25
37	Analytical computation	26
38	Walking trajectory	26
39	Input joint angles	27
40	Input joint angles 2	27
41	Ankle pitch	28
42	Ankle roll	28
43	Hip pitch	29
44	Hip roll	29
45	Knee	30
46	Robot motion	30

LIST OF TABLES

Table No.	Title	Page No.
1	D-H parameters of leg part of a humanoid robot	8

1. INTRODUCTION

Robots will become the new future because an aging society is coming and not everyone can afford to do regular tasks with utmost efficiency. To avoid human beings doing high risk tasks and risking their lives, robots will be the new normal for that. Replacing duplicating jobs and making their way onto educating children, robots will also come handy for people who want pets.

“Robots will soon become our part of day to day”
-Bill Gates

However,

Designing controllers for robots presents many challenges. While many researchers have been able to build functional robots, there is little consensus on how to control them. There is yet to be a walking robot that comes close to matching human skill. Meanwhile, robotic arms have been perfected to a stage where they can match or even surpass human skill for trajectory following tasks. In order for walking robotics to reach this stage, perhaps a new approach to legged robotics is necessary.

1.1 BACKGROUND

Although nearly every human understands what it feels like to walk, it is difficult to comprehend all the mechanisms that make walking possible. Many researchers have tackled this question, and some of their efforts have produced remarkable results. Two of today's premiere walking robots are ASIMO and Qrio, made by Honda and Sony, respectively. Both of these humanoid robots use a position control algorithm to move and rotate various limbs and joints similar to those used in robotic arms.

1.2 THE WALKING ROBOTICS CONTROL PROBLEM

Although ASIMO and Qrio appear to be the most human-like robots, the position controller requires an exorbitant amount of energy, far beyond that required by real human walking. Furthermore their movements are tense and shaky, and high precision is necessary in all motion. For these reasons, controlling a walking robot is a more complex problem than simple position control systems have been able to solve. A solution to this control problem requires exploring alternative controller designs.

1.3 THE MACHINE LEARNING HYPOTHESIS

One hypothesis is that machine learning may be used to control walking robots. Machine learning techniques are derived from a set of algorithms used to train neural networks in the human brain. The idea is that the robot can essentially learn how to walk given a simple set of initial conditions and a reward-based feedback controller. The possibility of using machine learning algorithms opens up the possibility of having an intelligent walking robot that learns how to walk in the same way that human toddlers learn how to walk. By exploring this possibility, walking robotics is moving in a new direction.

1.4 OBJECTIVE

Walking robotics and machine learning theory provide the backdrop for this project. The goal is to design and build a robot that can maneuver itself in every possible terrain and which is ideal for exploring the machine learning hypothesis.

1.5 WHY HUMANOID ROBOT

- Advantages

- A humanoid robot has a structure similar to human's leg and has higher mobility than conventional wheeled robots.
- Involves numerous fields.

- Disadvantages

- Balance should be concerned.
- Complicated to design mechanism.
- Has complex dynamics and many non-linear factors.
- It is very difficult to move a robot stably.

2. MECHANISM OF HUMANOID ROBOT

2.1 DESIGN OF MECHANISM OF LEG MOVEMENT

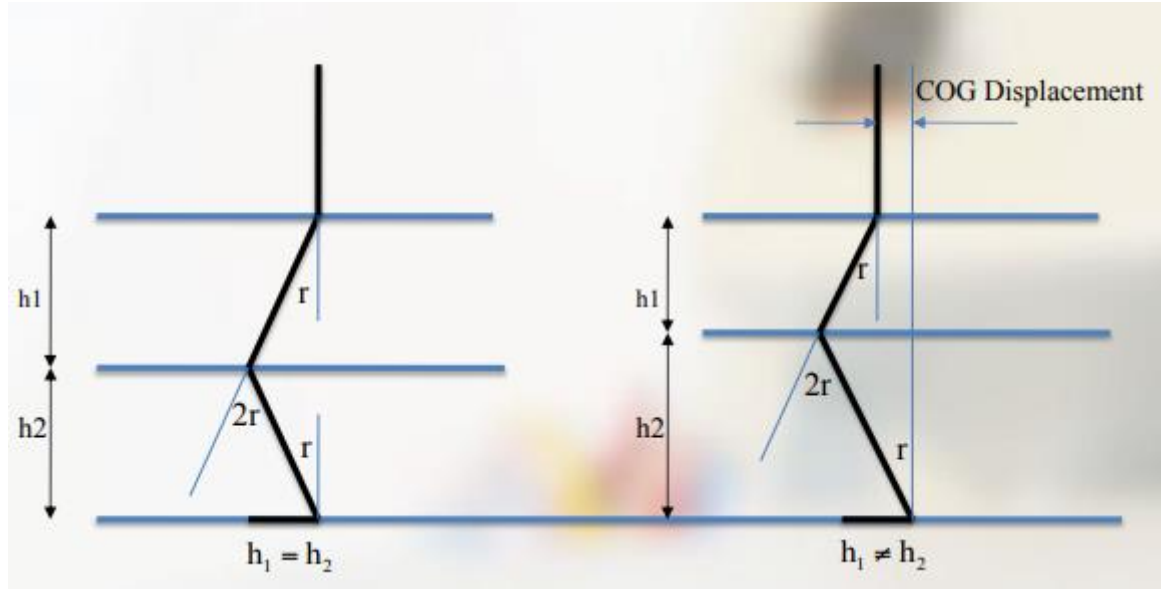


Fig 1: Different link length will cause displacement of CoG [13]

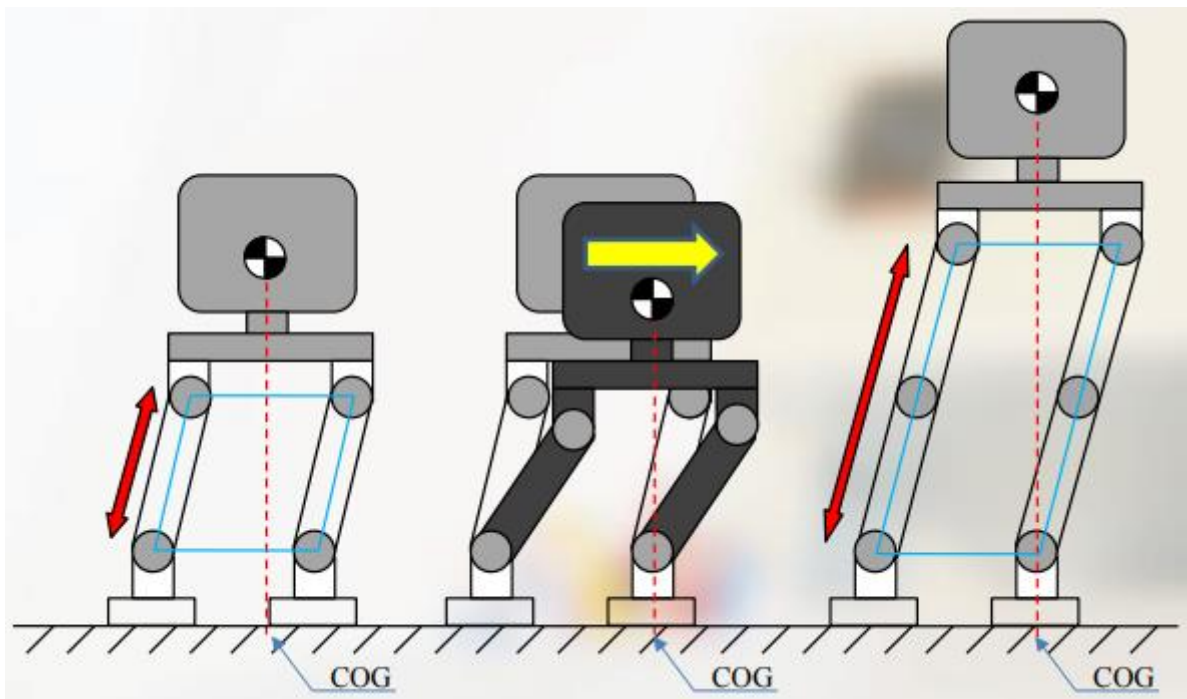


Fig 2: Different leg length will cause large displacement [13]

2.2 DESIGN OF MECHANISM OF ARM ARTICULATION

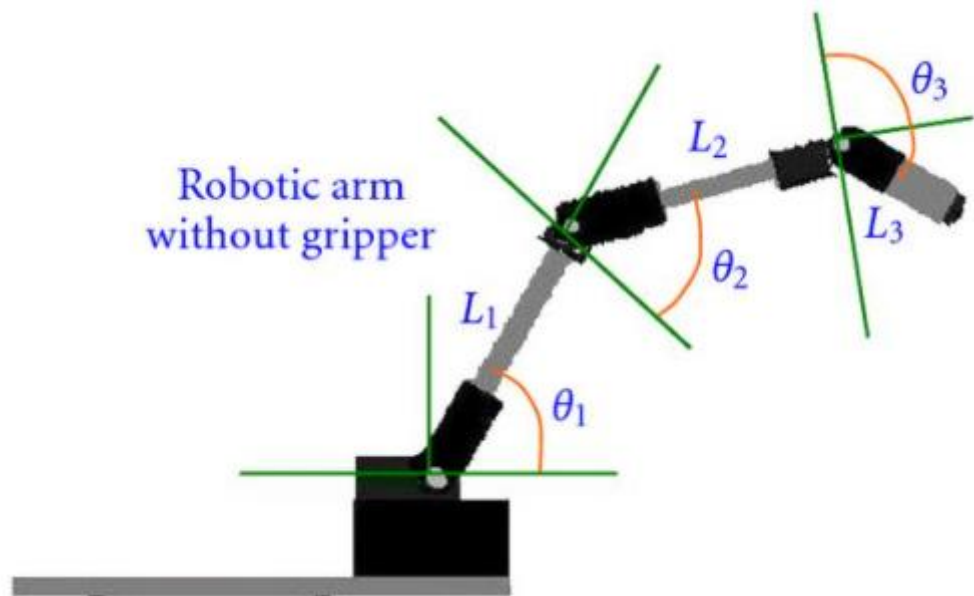


Fig 3: Arm joint angles ^[2]

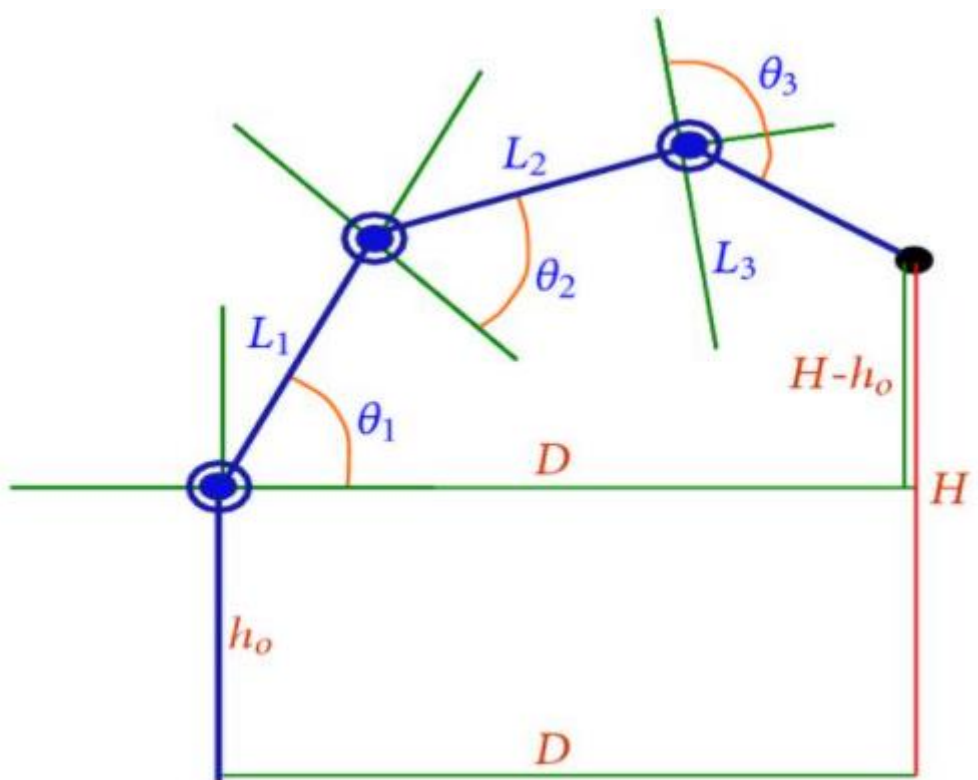


Fig 4: Arm joint geometric representation ^[2]

3. HARDWARE OF HUMANOID ROBOT

3.1 ACTUATORS

The whole trunk of robot is composed by 16 motors with different size based on required torque.

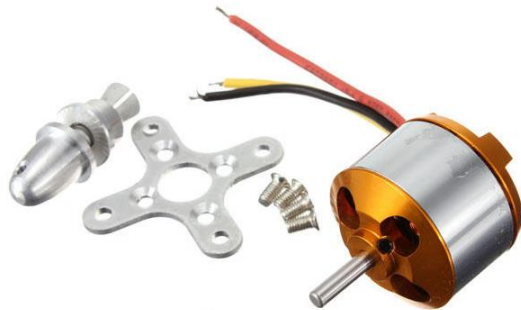


Fig 5: BLDC motor [3]

3.2 ACCELEROMETERS AND GYROSCOPES

The accelerometer has been converted to an acceleration that varies between -1 g and $+1\text{ g}$. The ADXRS300 is a complete angular rate sensor (gyroscope).



Fig 6: ADXRS300 [3]

3.3 FORCE SENSING RESISTOR

Exhibits a decrease in resistance with an increase in force applied normal to the device surface.

3.4 CMOS SENSOR

In practical situation high speed module without hyper speed processor will be in vain.



Fig 7: CMOS sensor [3]

3.5 EXTERNAL CIRCUITS

- Data acquisition circuit
- Power management circuit
- Isolation circuit
- Peripheral circuits

3.6 PROCESSOR

- Collects information
- Computes robot dynamic
- Performs human brain
- High hardware acceleration



Fig 8: Rasberry Pi 3B+ [3]

4. MODELLING AND REFERENCE TRAJECTORY PLANNING

4.1 FORWARD KINEMATICS

Determines the position and orientation of the end effector given the values for the joint variables of the robot.

The position sense of the twist angle and the joint angle are shown as below:

Forward kinematics

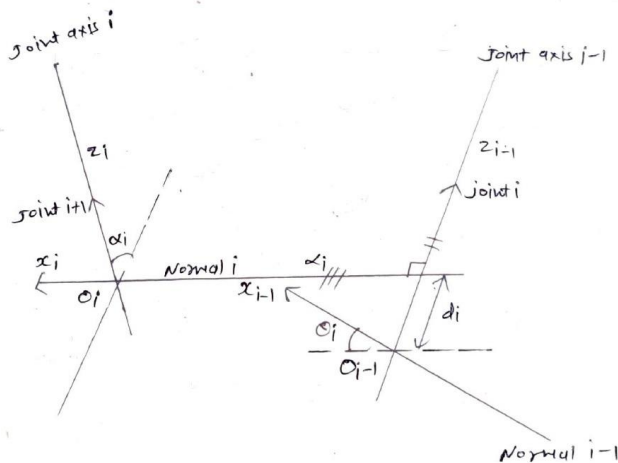


Fig 9: Position sense of twist angle [9]

The four principal homogeneous transforms are involved:

$${}^{i-1}\mathbf{H} = \mathbf{H}_{rz_{i-1},\theta_i} \mathbf{H}_{tz_{i-1},d_i} \mathbf{H}_{tx_i,a_i} \mathbf{H}_{ex_i,a_i}$$

Homogeneous transform parameters are defined in appendix C and is shown as

$${}^{i-1}\mathbf{H} = \begin{bmatrix} \cos \theta_i & -\cos \alpha_i \sin \theta_i & \sin \alpha_i \sin \theta_i & a_i \cos \theta_i \\ \sin \theta_i & \cos \alpha_i \cos \theta_i & -\sin \alpha_i \cos \theta_i & a_i \sin \theta_i \\ 0 & \sin \alpha_i & \cos \alpha_i & d_i \\ 0 & 0 & 0 & 1 \end{bmatrix}$$

For simplicity, the homogeneous transform denotes as ${}^i\mathbf{H} = \mathbf{A}_i$

The end-link expressed by the homogeneous transform is

$${}_n^0\mathbf{H}(\mathbf{q}) = {}_1^0\mathbf{H}(q_1) {}_2^1\mathbf{H}(q_2) \dots {}_{n-1}^n\mathbf{H}(q_n) = \mathbf{A}_1 \mathbf{A}_2 \dots \mathbf{A}_n$$

, where $\mathbf{q} = [q_1 \ q_2 \ \dots \ q_n]^T$

Table- 1: D-H parameters of leg part of a humanoid robot [1]

Joint i	α_i	a_i	d_i	θ_i
1	$\pi/2$	0	0	θ_1
2	0	a_3	0	θ_2
3	0	a_2	0	θ_3
4	$-\pi/2$	0	0	θ_4
5	$-\pi/2$	0	0	θ_5
6	0	a_1	0	θ_6

Leg part of a humanoid robot is given by

$${}^0\mathbf{H}(\mathbf{q}) = {}^0\mathbf{H}(q_1) {}^1\mathbf{H}(q_2) {}^2\mathbf{H}(q_3) {}^3\mathbf{H}(q_4) {}^4\mathbf{H}(q_5) {}^5\mathbf{H}(q_6) = \mathbf{A}_1\mathbf{A}_2\mathbf{A}_3\mathbf{A}_4\mathbf{A}_5\mathbf{A}_6$$

The D-H parameters form is shown as

$${}^0\mathbf{H}(\mathbf{q}) = \begin{bmatrix} n_x & o_x & a_x & p_x \\ n_y & o_y & a_y & p_y \\ n_z & o_z & a_z & p_z \\ 0 & 0 & 0 & 1 \end{bmatrix}$$

, where

$$\begin{aligned} o_y &= (s_1 c_{234} s_5 - c_1 c_5) s_6 + s_1 s_{234} c_6 \\ o_z &= s_{234} s_5 s_6 - c_{234} c_6 \\ a_x &= -c_1 c_{234} c_5 + s_1 s_5 \\ a_y &= -s_1 c_{234} c_5 - c_1 s_5 \\ a_z &= -s_{234} c_5 \\ p_x &= -a_1 (c_1 c_{234} s_5 + s_1 c_5) c_6 + a_1 c_1 s_{234} s_6 + c_1 (a_2 c_{23} + a_3 c_2) \\ p_y &= a_1 (-s_1 c_{234} s_5 + c_1 c_5) c_6 + a_1 s_1 s_{234} s_6 + s_1 (a_2 c_{23} + a_3 c_2) \\ p_z &= -a_1 s_{234} s_5 c_6 - a_1 c_{234} s_6 + a_2 s_{23} + a_3 s_2 \\ n_x &= (-c_1 c_{234} s_5 - s_1 s_5) c_6 + c_1 s_{234} s_6 \\ n_y &= (-s_1 c_{234} s_5 + c_1 c_5) c_6 + s_1 s_{234} s_6 \\ n_z &= -s_{234} s_5 c_6 - c_{234} s_6 \\ o_x &= (c_1 c_{234} s_5 + s_1 c_5) s_6 + c_1 s_{234} c_6 \end{aligned}$$

Whenever convenient shorthand notation defines as

$s_\theta = \sin \theta$ And $c_{\psi+\varphi} = \cos (\psi + \varphi)$ for trigonometric functions.

4.2 INVERSE KINEMATICS

Determine the values for the joint variables given the end effector's position and orientation.

One sub chain which comprises joint variables $\theta_1, \theta_2, \theta_3$

$\theta_1 = \text{Atan } 2(y_c, x_c)$ In which Atan2(y, x) denotes the two argument arctangent function.

Applying the cosine theorem to obtain

$$\cos \theta_3 = \frac{x_c^2 + y_c^2 + z_c^2 - a_2^2 - a_3^2}{2a_2a_3}$$

Hence θ_3 is given by

$$\theta_3 = \text{Atan } 2(\pm\sqrt{1 - \cos^2 \theta_3}, \cos \theta_3)$$

Similarly θ_2 is given by

$$\theta_2 = \text{Atan } 2(z_c, \sqrt{x_c^2 + y_c^2}) + \text{Atan } 2(a_2 \sin \theta_3, a_3 + a_2 \cos \theta_3)$$

Hence θ_5 is given by

$$\theta_5 = \text{Atan } 2(s_1 r_{13} - c_1 r_{23}, \pm\sqrt{1 - (s_1 r_{13} - c_1 r_{23})^2})$$

Then θ_4 and θ_6 are given respectively as

$$\theta_6 = \text{Atan } 2(s_1 r_{12} - c_1 r_{22}, -s_1 r_{11} + c_1 r_{21})$$

$$\theta_4 = \text{Atan } 2(-c_1 s_{23} r_{13} - s_1 s_{23} r_{23} + c_{23} r_{33}, c_1 c_{23} r_{13} + s_1 c_{23} r_{23} + s_{23} r_{33})$$

It will get 8 different solutions. Preserve the one solution by determining movable range.

4.3 ZERO MOMENT POINT

If ZMP is in the stable region for double support phase and single support phase, then the robot will not go falling down situation.

$$x_{zmp} = \frac{\sum_{i=1}^n m_i(\ddot{z}_i - g_z)x_i - \sum_{i=1}^n m_i(\ddot{x}_i - g_x)z_i}{\sum_{i=1}^n m_i(\ddot{z}_i - g_z)}$$

$$y_{zmp} = \frac{\sum_{i=1}^n m_i(\ddot{z}_i - g_z)y_i - \sum_{i=1}^n m_i(\ddot{y}_i - g_y)z_i}{\sum_{i=1}^n m_i(\ddot{z}_i - g_z)}$$

, where $\mathbf{P} = [p_x, p_y, p_z]^T$ represents the ZMP vector, m_i is the each link

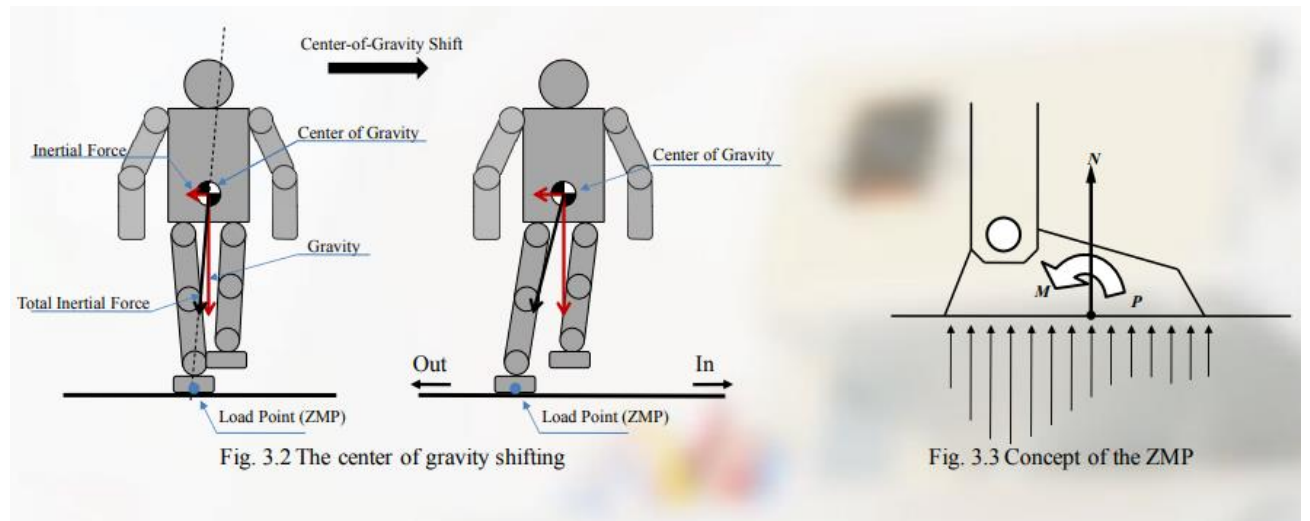


Fig 10: Zero Moment Point ^[13]

Thus the actual ZMP can be computed by

$$\mathbf{P}_{\text{ZMP}} = \frac{\sum_{i=1}^n f_i \mathbf{r}_i}{\sum_{i=1}^n f_i}$$

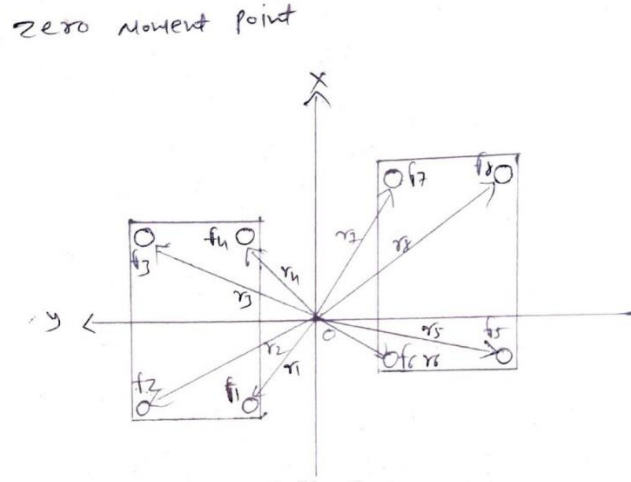


Fig 11: Actual ZMP [9]

4.4 LINEAR INVERTED PENDULUM MODEL

To extract a dominant feature which is high-order and nonlinear and to use this dominant factor to explain the dynamics of the system.

The position of the body can be calculated via the moment of mass equation:

$$m\mathbf{r}_c = \sum_{k=1}^n m_k \mathbf{r}_k$$

, where \mathbf{r}_k is the position of the k^{th} particle, $m = \sum_{k=1}^n m_k$ is the total mass.

linear inverted pendulum model (LIPM)

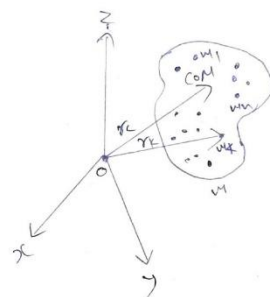


Fig 12: LIPM [9]

The dynamics equations of the inverted pendulum can be derived as follows:

$$p_x = \frac{m(\ddot{c}_z - g)c_x - m\ddot{c}_x c_z}{m(\ddot{c}_z - g)}$$

$$p_y = \frac{m(\ddot{c}_z - g)c_y - m\ddot{c}_y c_z}{m(\ddot{c}_z - g)}$$

To attain linear equations assume the z-coordinates of the inverted pendulum to be constant

$$p_x = c_x - \frac{z_c}{g} \ddot{c}_x$$

$$p_y = c_y - \frac{z_c}{g} \ddot{c}_y$$

4.5 TABLE CART MODEL

The moment around the ZMP must be zero the following condition hold.

$$\tau_{zmp} = mg(x - p_x) - m\ddot{x}z_c = 0$$

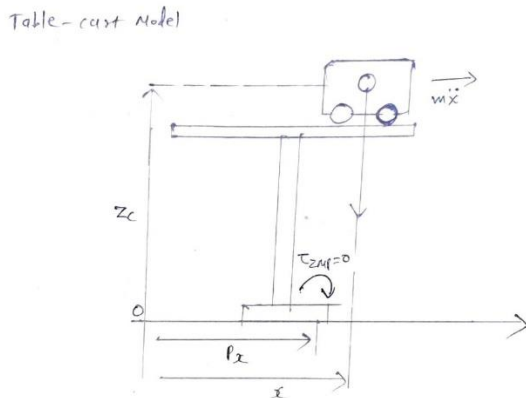


Fig 13: Table cart model [9]

4.6 FOURIER APPROXIMATION OF COM TRAJECTORIES

The ZMP reference trajectories can be expressed as follows:

$$p_x^{ref}(t) = L \sum_{k=1}^{\infty} u(t - kT_0)$$

$$p_y^{ref}(t) = B \cdot u(t) + 2B \sum_{k=1}^{\infty} (-1)^k \cdot u(t - kT_0)$$

Finally, the CoM can be obtained by applying inverse Laplace transformations as follows:

$$c_x(t) = L \sum_{k=0}^{\infty} [1 - \cosh \omega_n(t - kT_0)] \cdot 1(t - kT_0)$$

$$c_x(t) = 2B \sum_{k=0}^{\infty} (-1)^k [1 - \cosh \omega_n(t - kT_0)] \cdot 1(t - kT_0)$$

Assuming the reference trajectory of CoM has the form by using Fourier series. As a result, the x-directional reference trajectory of CoM can be found as follows:

$$c_x^{ref}(t) = \frac{L}{T_0} \left(t - \frac{T_0}{2} \right) + \sum_{n=1}^{\infty} \left[\frac{LT_0^2 \omega_n^2 (1 + \cos n\pi)}{n\pi(T_0^2 \omega_n^2 + n^2\pi^2)} \sin \left(\frac{n\pi}{T_0} t \right) \right]$$

The y-directional reference trajectory of CoM can be found in a similar manner as follows:

$$c_y^{ref}(t) = \sum_{n=1}^{\infty} \left[\frac{2BT_0^2 \omega_n^2 (1 - \cos n\pi)}{n\pi(T_0^2 \omega_n^2 + n^2\pi^2)} \sin \left(\frac{n\pi}{T_0} t \right) \right]$$

4.7 SWING FOOT REFERENCE TRAJECTORIES

The hip joint fix on the same height. The movement trajectories show in below:

$$x_f(t) = \frac{L}{\pi} \left[2\pi \frac{t}{T_s} - \sin \left(2\pi \frac{t}{T_s} \right) \right]$$

$$y_f(t) = \pm B$$

$$z_f(t) = \frac{h_f}{2} \left[1 - \cos \left(2\pi \frac{t}{T_s} \right) \right]$$

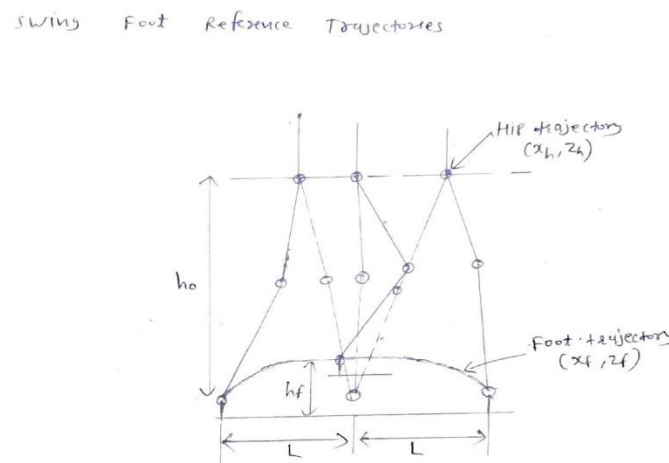


Fig 14: Swing foot reference trajectories [9]

5. DESIGN OF PARTS AND ASSEMBLIES

5.1 ACTUATOR BASE

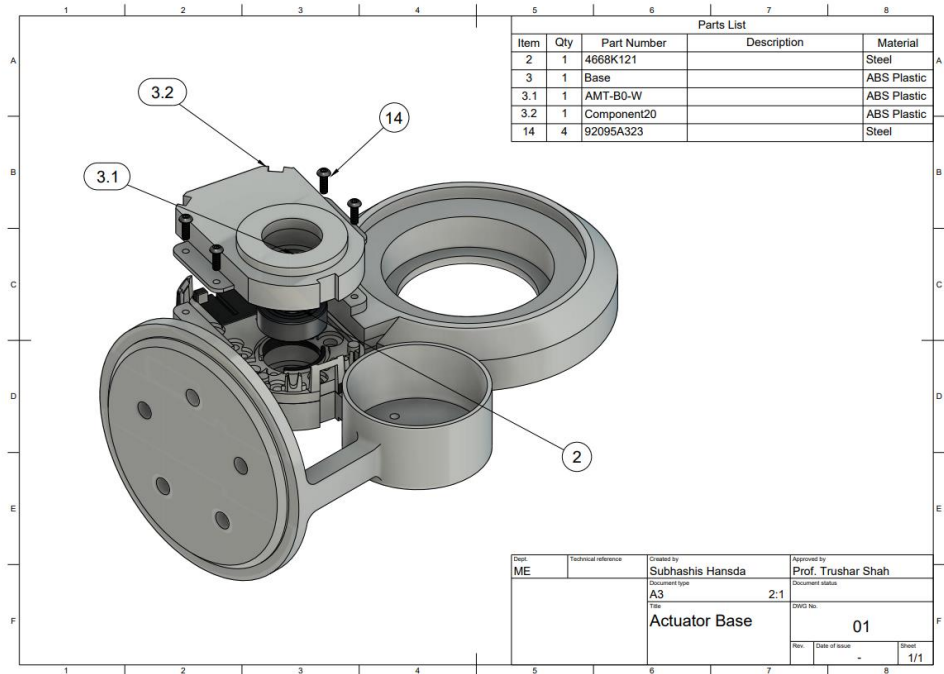


Fig 15: Design of actuator base

5.2 ACTUATOR JOINT TOP

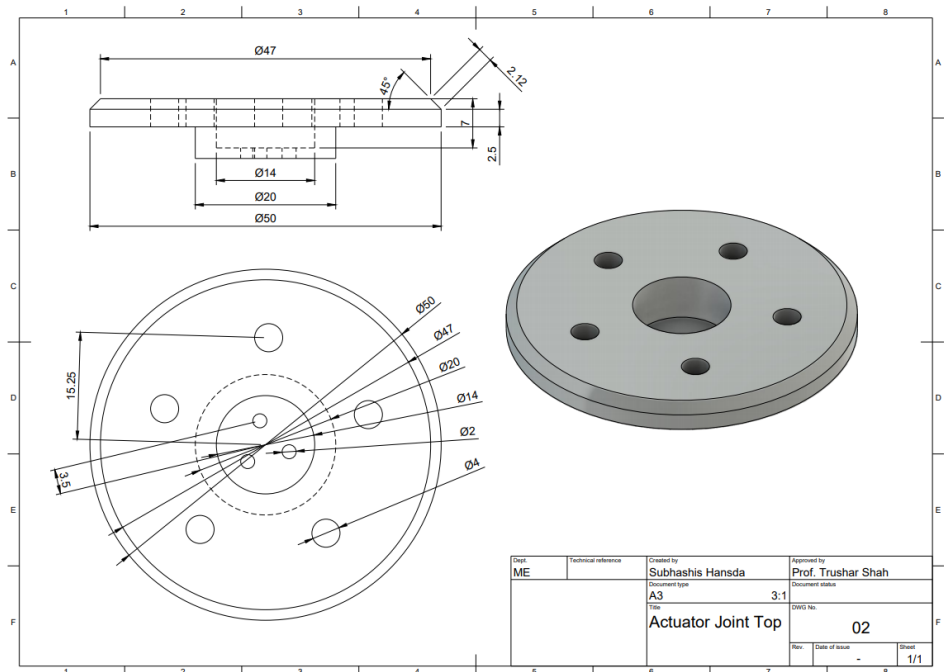


Fig 16: Design of actuator joint top

5.3 ACTUATOR JOINT BOTTOM

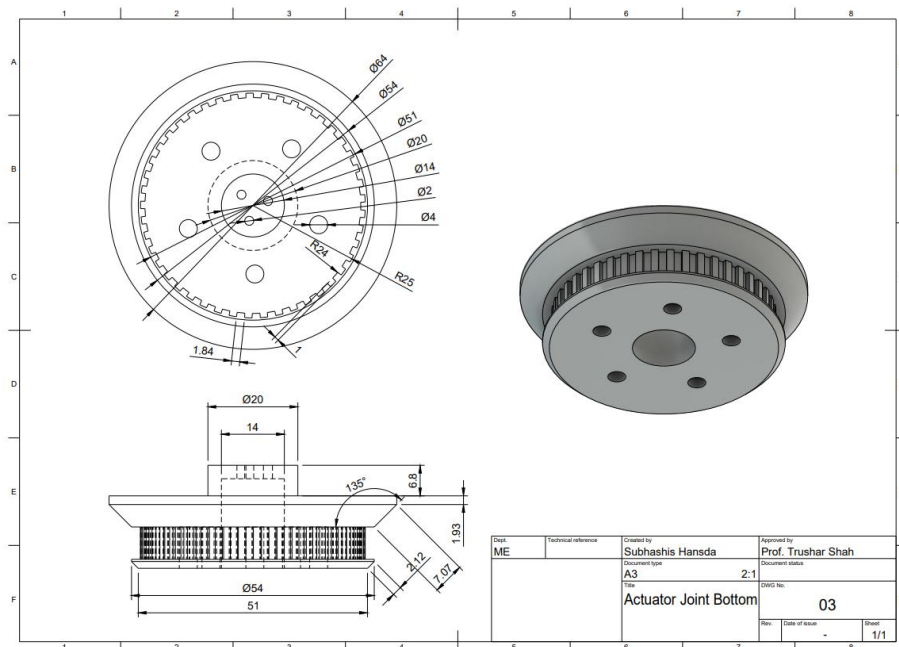


Fig 17: Design of actuator joint bottom

5.4 ACTUATOR ASSEMBLY

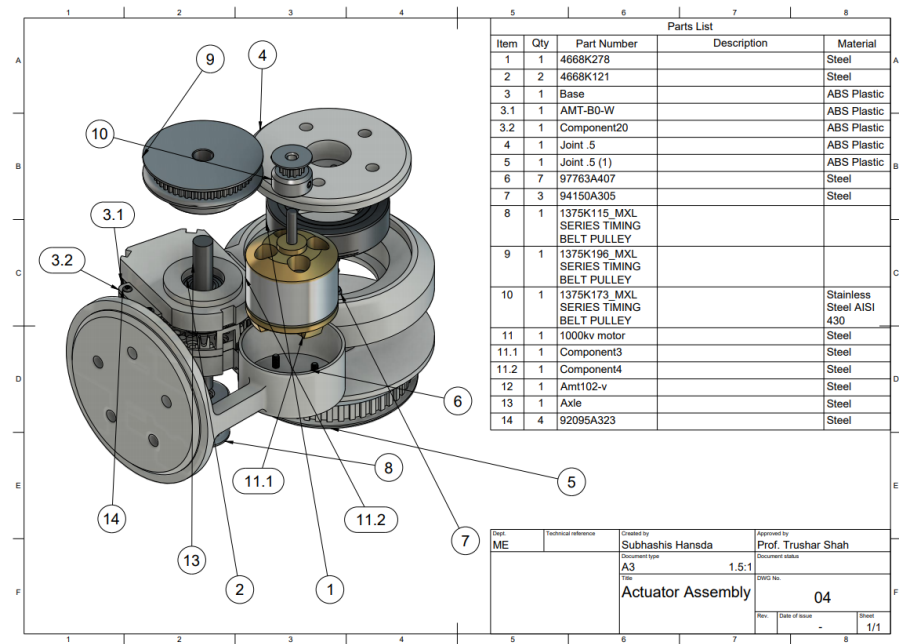


Fig 18: Design of actuator assembly

5.5 HAND UPPER ARM

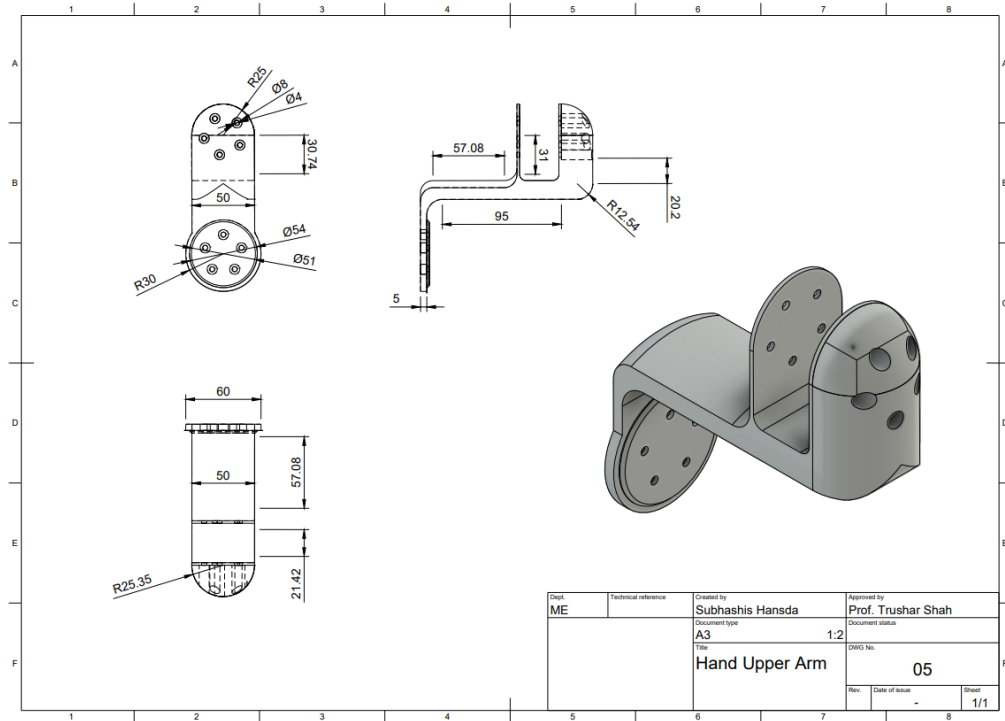


Fig 19: Design of hand upper arm

5.6 HAND LOWER ARM

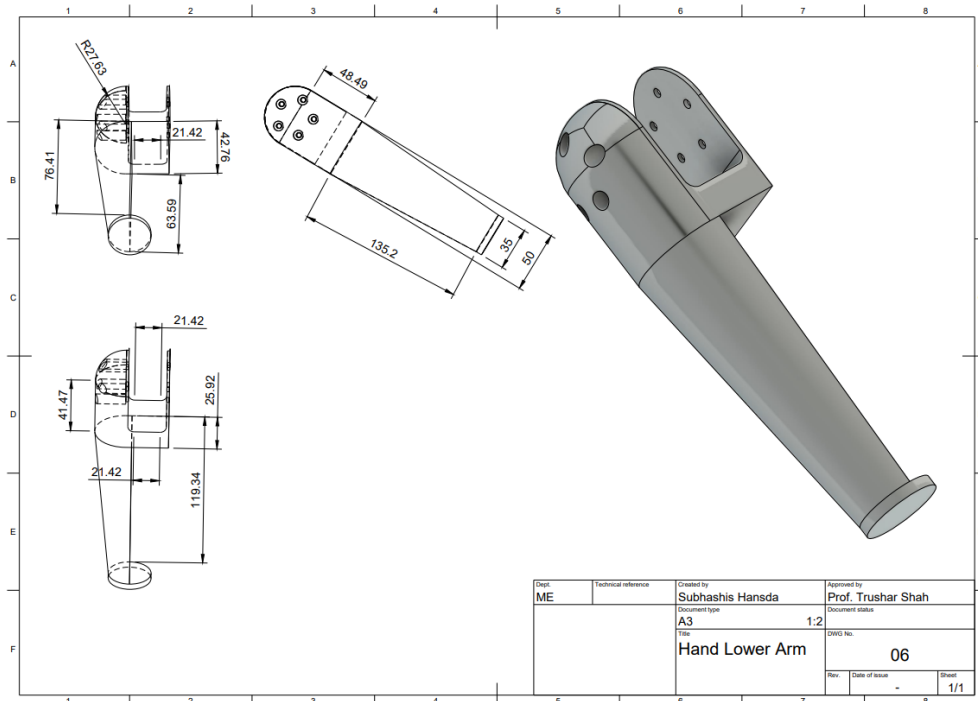


Fig 20: Design of hand lower arm

5.7 HAND ASSEMBLY

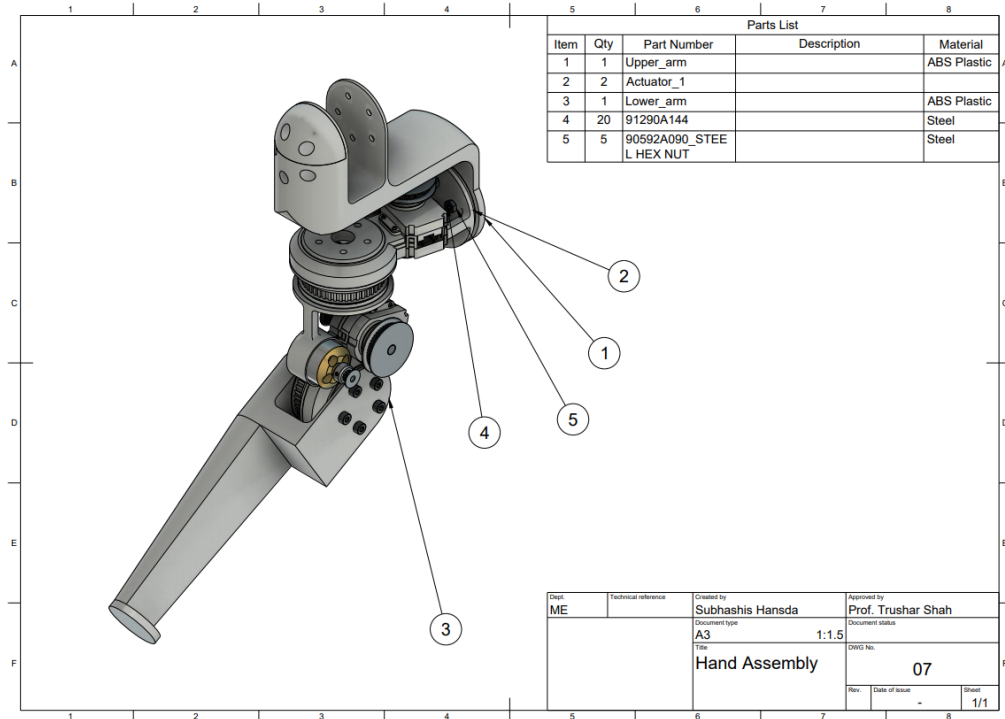


Fig 21: Design of hand assembly

5.8 LEG UPPER

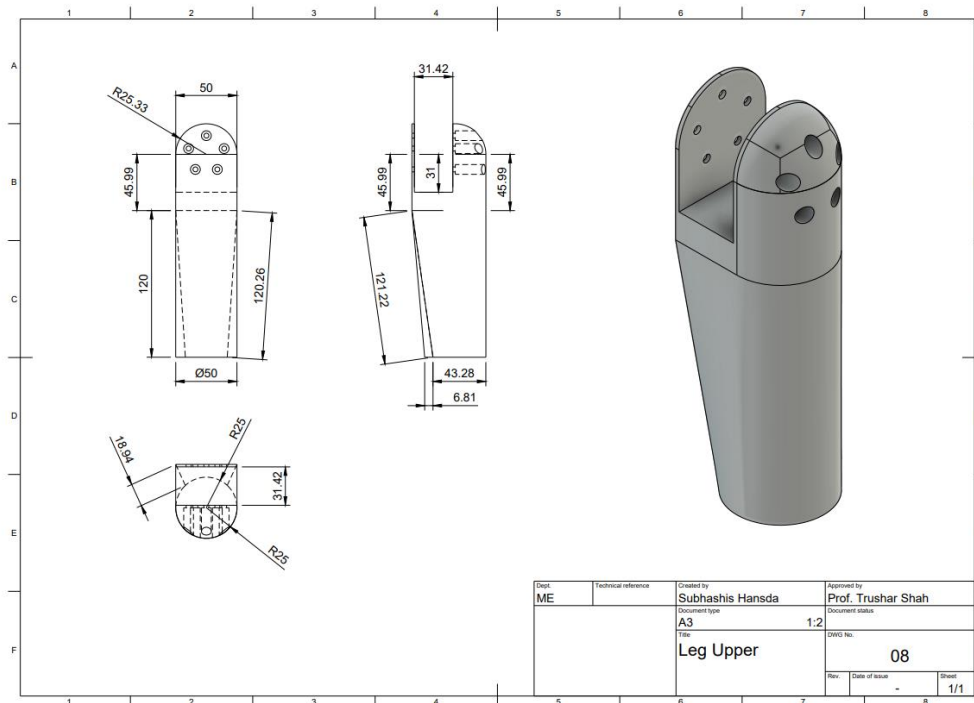


Fig 22: Design of leg upper

5.9 LEG LOWER

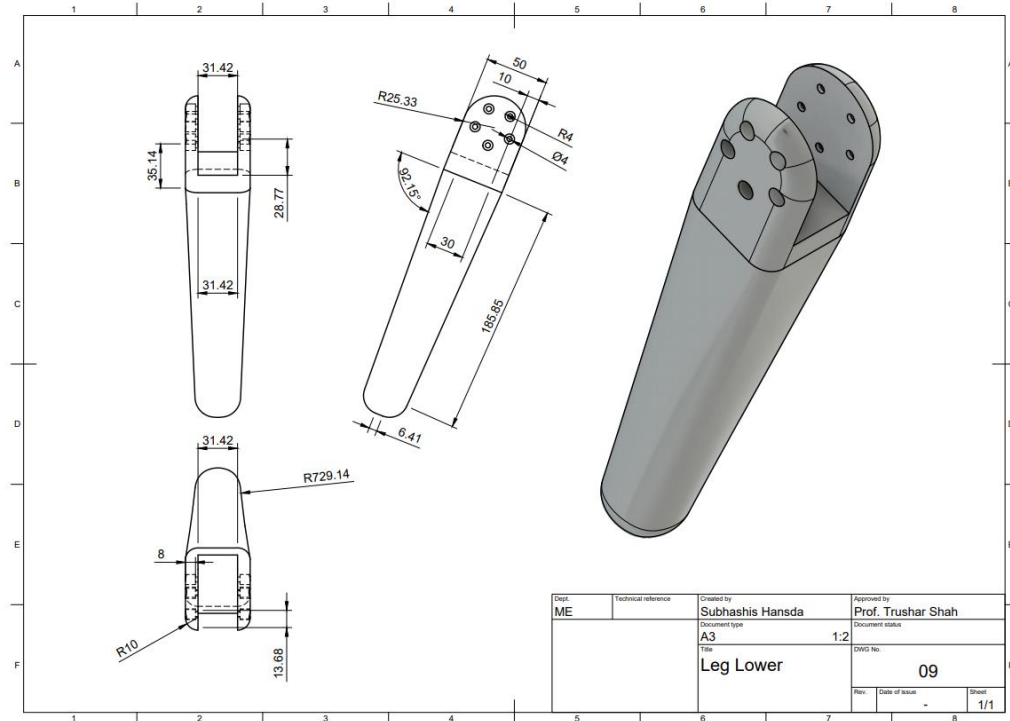


Fig 23: Design of leg lower

5.10 LEG ASSEMBLY

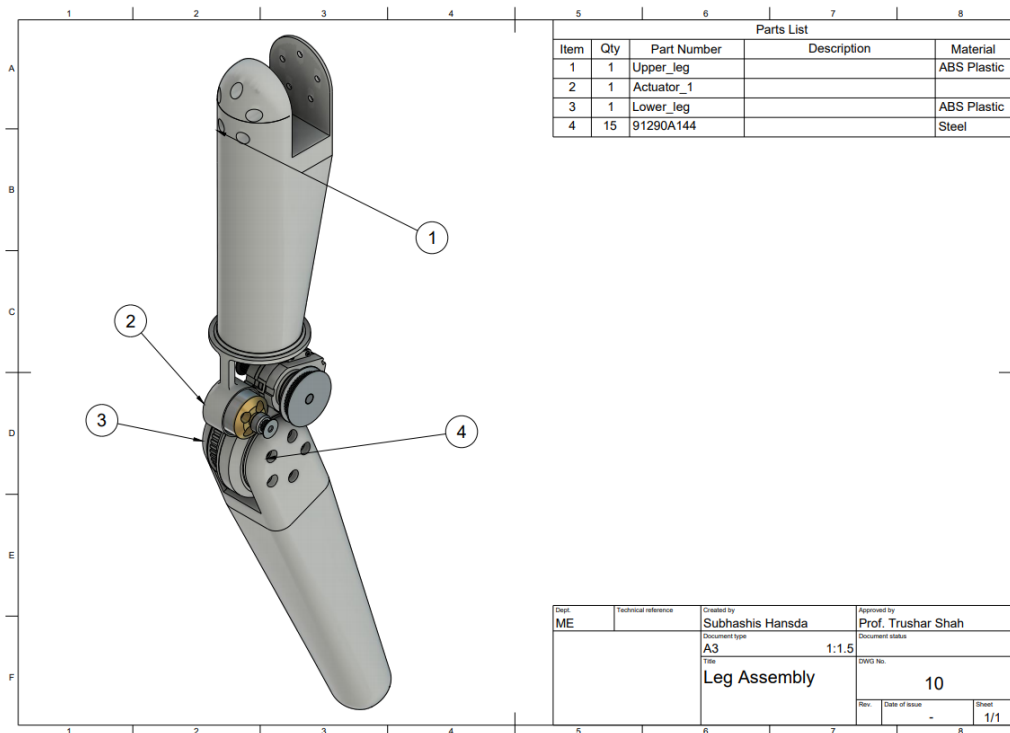


Fig 24: Design of leg assembly

5.11 CHEST UPPER BODY

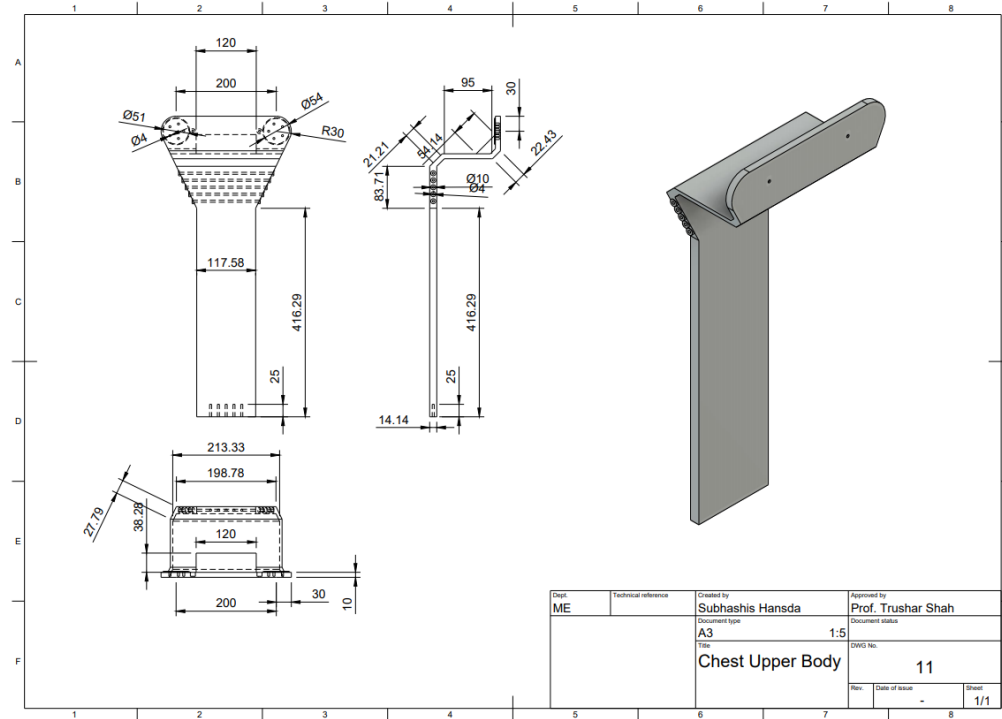


Fig 25: Design of chest upper body

5.12 CHEST LOWER BODY

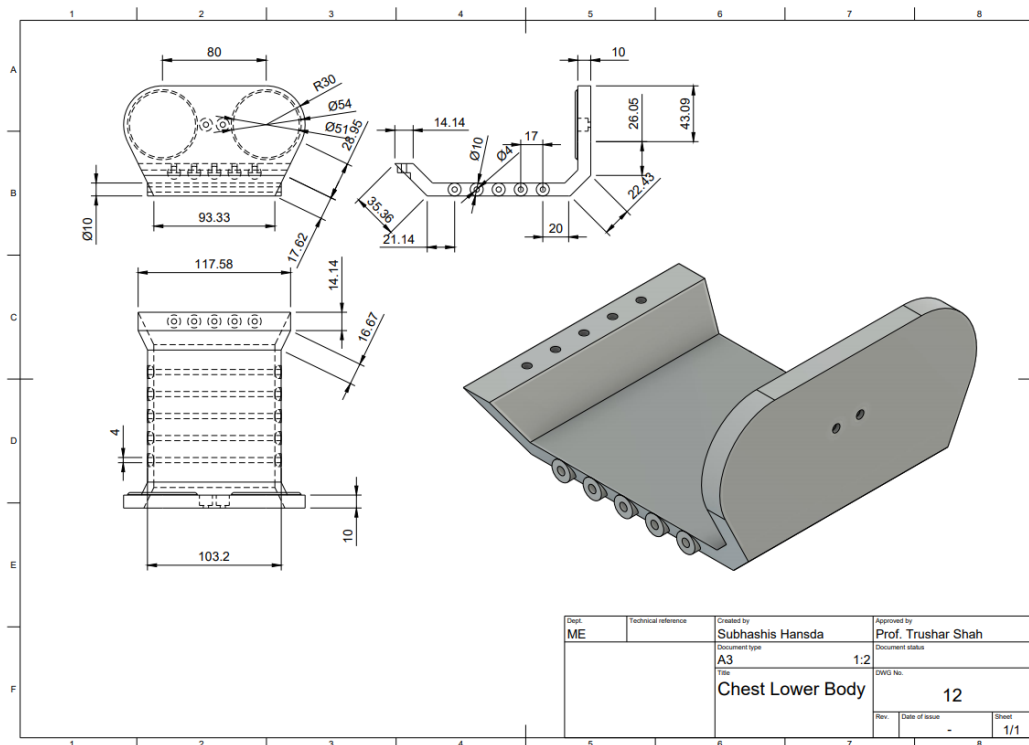


Fig 26: Design of chest lower body

5.13 CHEST UPPER LINK

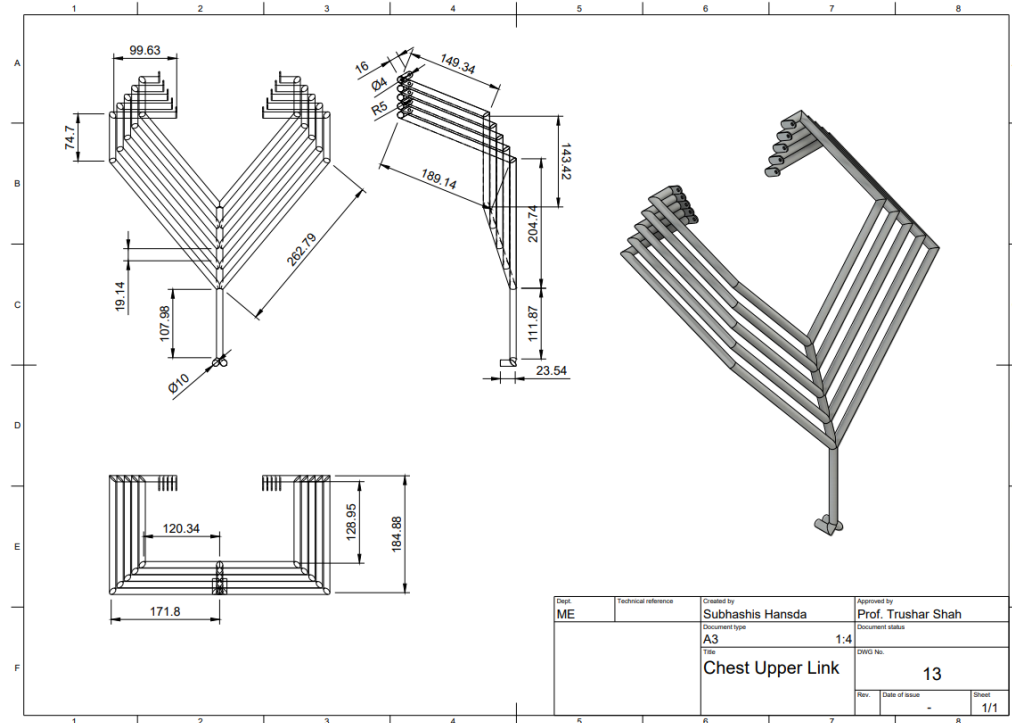


Fig 27: Design of chest upper link

5.14 CHEST LOWER LINK

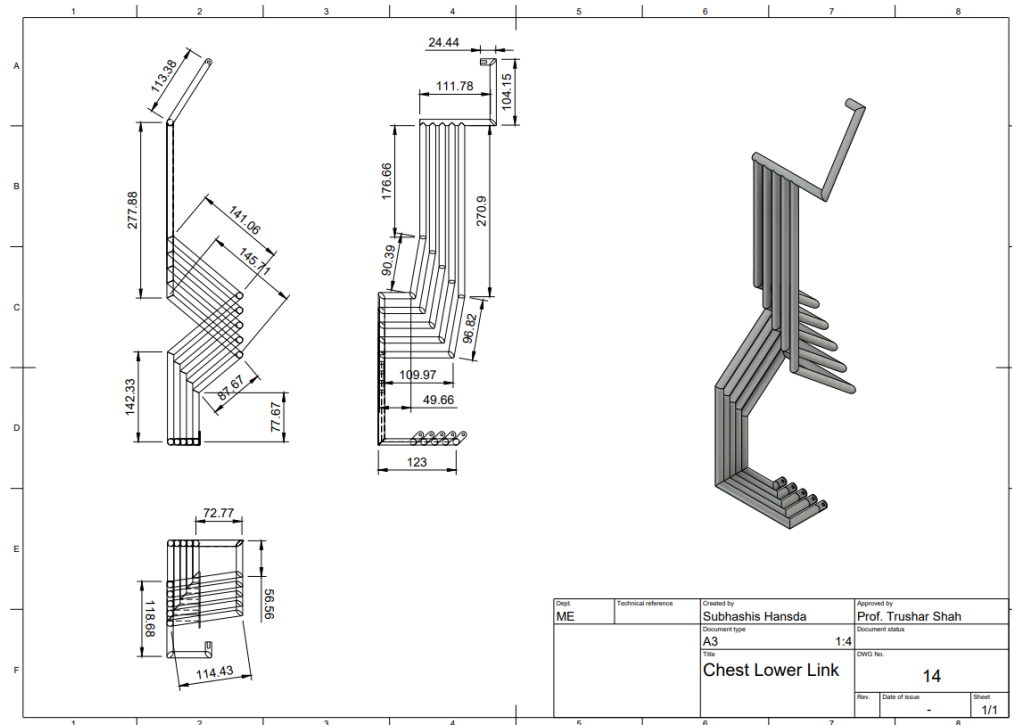


Fig 28: Design of chest lower link

5.15 CHEST ASSEMBLY

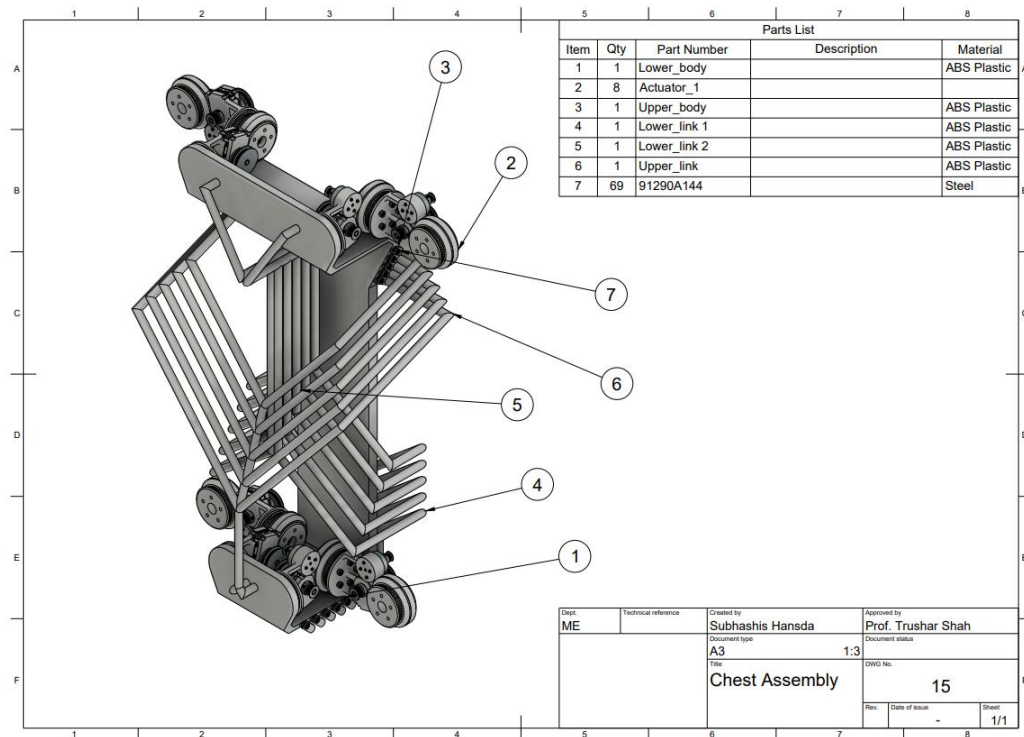


Fig 29: Design of chest assembly

Actuator Base Analysis

Analyzed File	actuator_1 v55
Version	Autodesk Fusion 360 (2.0.9313)
Creation Date	2020-12-04, 01:53:59
Author	

Project Properties

Title	Studies
Author	VAGUE

Simulation Model 1:1

Study 1 - Static Stress

Study Properties

Study Type	Static Stress
Last Modification Date	2020-12-04, 01:36:19

Settings

General

Contact Tolerance	0.1 mm
Remove Rigid Body Modes	No

Damping

Mesh

Average Element Size (% of model size)	
Solids	10
Scale Mesh Size Per Part	No
Average Element Size (absolute value)	-
Element Order	Parabolic
Create Curved Mesh Elements	Yes
Max. Turn Angle on Curves (Deg.)	60
Max. Adjacent Mesh Size Ratio	1.5
Max. Aspect Ratio	10
Minimum Element Size (% of average size)	20

Adaptive Mesh Refinement

Number of Refinement Steps	0
Results Convergence Tolerance (%)	20
Portion of Elements to Refine (%)	10
Results for Baseline Accuracy	Von Mises Stress

Materials

Component	Material	Safety Factor
base:1	ABS Plastic	Yield Strength

ABS Plastic

Density	1.06E-06 kg / mm ³
Young's Modulus	2240 MPa
Poisson's Ratio	0.38
Yield Strength	20 MPa
Ultimate Tensile Strength	29.6 MPa
Thermal Conductivity	1.6E-04 W / (mm C)
Thermal Expansion Coefficient	8.57E-05 / C
Specific Heat	1500 J / (kg C)

Contacts

Mesh

Type	Nodes	Elements

Solids 11565 6312

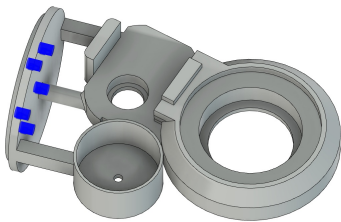
□ Load Case1

□ Constraints

□ Fixed1

Type	Fixed
Ux	Yes
Uy	Yes
Uz	Yes

□ Selected Entities

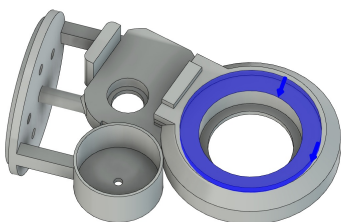


□ Loads

□ Force1

Type	Force
Magnitude	11 N
X Value	11 N
Y Value	0.005635 N
Z Value	0 N
X Angle	-75 deg
Y Angle	-90 deg
Z Angle	0 deg
Force Per Entity	No

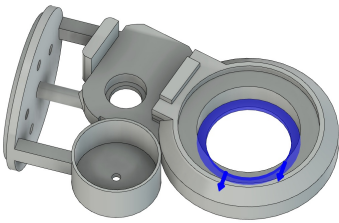
□ Selected Entities



□ Force2

Type	Force
Magnitude	11 N
X Value	11 N
Y Value	0 N
Z Value	-1.618E-15 N
X Angle	-270 deg
Y Angle	0 deg
Z Angle	0 deg
Force Per Entity	No

□ Selected Entities



□ Results

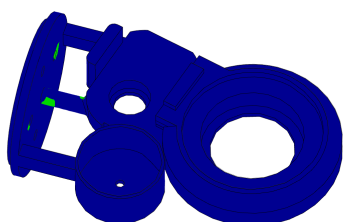
□ Result Summary

Name	Minimum	Maximum
Safety Factor		
Safety Factor (Per Body)	3.093	15
Stress		
Von Mises	0.003179 MPa	6.466 MPa
1st Principal	-3.702 MPa	11.52 MPa
3rd Principal	-10.66 MPa	4.651 MPa
Normal XX	-9.849 MPa	10.32 MPa
Normal YY	-6.552 MPa	5.993 MPa
Normal ZZ	-5.633 MPa	5.914 MPa
Shear XY	-2.487 MPa	2.154 MPa
Shear YZ	-1.543 MPa	1.623 MPa
Shear ZX	-2.289 MPa	2.041 MPa
Displacement		
Total	0 mm	0.4422 mm
X	-0.01305 mm	0.381 mm
Y	-0.1234 mm	0.09382 mm
Z	-0.07956 mm	0.2411 mm
Reaction Force		
Total	0 N	7.296 N
X	-6.106 N	5.948 N
Y	-4.166 N	2.516 N
Z	-2.725 N	2.771 N
Strain		
Equivalent	1.987E-06	0.004272
1st Principal	1.425E-06	0.004684
3rd Principal	-0.004517	-1.259E-06
Normal XX	-0.002809	0.002588
Normal YY	-0.002702	0.002069
Normal ZZ	-0.001048	8.415E-04
Shear XY	-0.003064	0.002654
Shear YZ	-0.001901	0.002
Shear ZX	-0.00282	0.002515

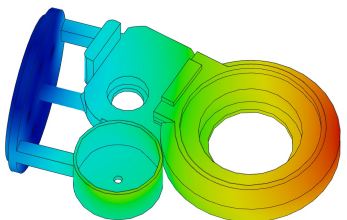
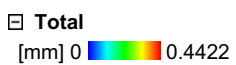
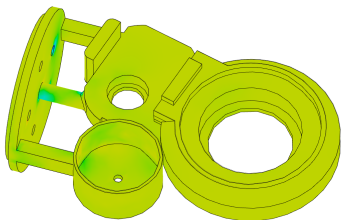
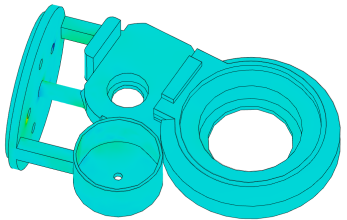
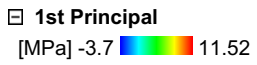
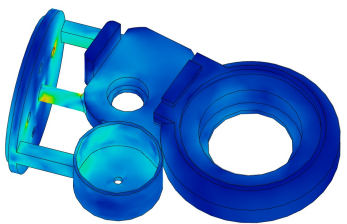
□ Safety Factor

□ Safety Factor (Per Body)

0 8



□ Stress



Actuator Joint Analysis

Analyzed File	actuator_1 v61
Version	Autodesk Fusion 360 (2.0.9313)
Creation Date	2020-12-04, 02:11:15
Author	

Project Properties

Title	Studies
Author	VAGUE

Simulation Model 1:1

Study 1 - Static Stress

Study Properties

Study Type	Static Stress
Last Modification Date	2020-12-04, 02:02:59

Settings

General

Contact Tolerance	0.1 mm
Remove Rigid Body Modes	No

Damping

Mesh

Average Element Size (% of model size)	
Solids	10
Scale Mesh Size Per Part	No
Average Element Size (absolute value)	-
Element Order	Parabolic
Create Curved Mesh Elements	Yes
Max. Turn Angle on Curves (Deg.)	60
Max. Adjacent Mesh Size Ratio	1.5
Max. Aspect Ratio	10
Minimum Element Size (% of average size)	20

Adaptive Mesh Refinement

Number of Refinement Steps	0
Results Convergence Tolerance (%)	20
Portion of Elements to Refine (%)	10
Results for Baseline Accuracy	Von Mises Stress

Materials

Component	Material	Safety Factor
joint .5 (1):1	ABS Plastic	Yield Strength
joint .5:1	ABS Plastic	Yield Strength

ABS Plastic

Density	1.06E-06 kg / mm ³
Young's Modulus	2240 MPa
Poisson's Ratio	0.38
Yield Strength	20 MPa
Ultimate Tensile Strength	29.6 MPa
Thermal Conductivity	1.6E-04 W / (mm C)
Thermal Expansion Coefficient	8.57E-05 / C
Specific Heat	1500 J / (kg C)

Contacts

Bonded

Name
[S] Bonded1 [joint .5 (1):1 joint .5:1]

Mesh

Type	Nodes	Elements
Solids	19084	11528

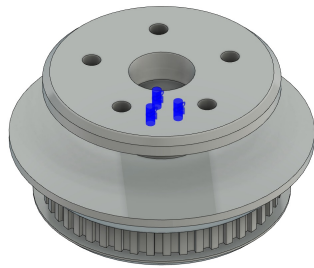
Load Case1

Constraints

Fixed1

Type	Fixed
Ux	Yes
Uy	Yes
Uz	Yes

Selected Entities

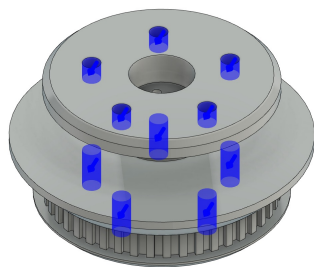


Loads

Force1

Type	Force
Magnitude	155 N
X Value	-64.06 N
Y Value	-141.1 N
Z Value	0 N
X Angle	0 deg
Y Angle	0 deg
Z Angle	0 deg
Force Per Entity	No

Selected Entities



Results

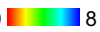
Result Summary

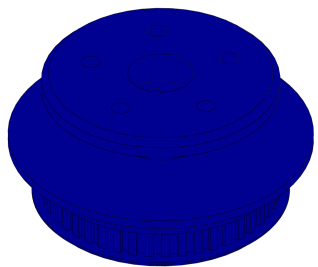
Name	Minimum	Maximum
Safety Factor		
Safety Factor (Per Body)	3.015	15
Stress		
Von Mises	0.001453 MPa	6.635 MPa
1st Principal	-3.527 MPa	10.7 MPa
3rd Principal	-9.674 MPa	4.152 MPa

Normal XX	-6.063 MPa	6.23 MPa
Normal YY	-7.354 MPa	8.545 MPa
Normal ZZ	-5.034 MPa	5.625 MPa
Shear XY	-3.237 MPa	2.749 MPa
Shear YZ	-2.485 MPa	1.353 MPa
Shear ZX	-1.652 MPa	0.9878 MPa
Displacement		
Total	0 mm	0.0704 mm
X	-0.02205 mm	5.63E-04 mm
Y	-0.04689 mm	1.957E-04 mm
Z	-0.0614 mm	0.06177 mm
Reaction Force		
Total	0 N	701.7 N
X	-6.389 N	7.782 N
Y	-11.24 N	13.44 N
Z	-511.7 N	701.7 N
Strain		
Equivalent	1.18E-06	0.004796
1st Principal	7.974E-07	0.005208
3rd Principal	-0.00503	-7.228E-07
Normal XX	-0.001682	0.001806
Normal YY	-0.002326	0.002057
Normal ZZ	-0.001348	0.001357
Shear XY	-0.003989	0.003387
Shear YZ	-0.003062	0.001667
Shear ZX	-0.002036	0.001217
Contact Pressure		
Total	0 MPa	4.367 MPa
X	-1.286 MPa	1.294 MPa
Y	-1.496 MPa	1.163 MPa
Z	-4.367 MPa	4.065 MPa

Safety Factor

Safety Factor (Per Body)

0  8



Stress

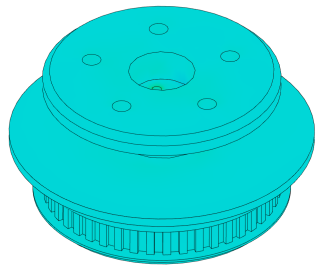
Von Mises

[MPa] 0.001  6.635

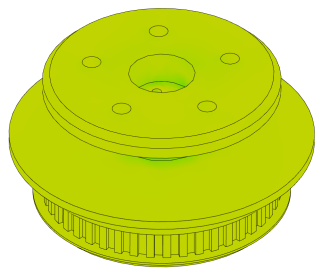


1st Principal

[MPa] -3.53  10.7

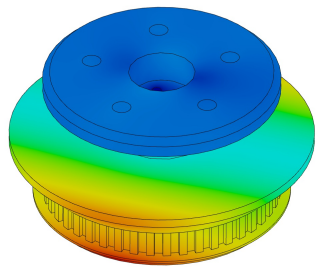


3rd Principal
[MPa] -9.674 4.152



Displacement

Total
[mm] 0 0.0704



Chest Lower Body Analysis

Analyzed File	chest_2 v47
Version	Autodesk Fusion 360 (2.0.9313)
Creation Date	2020-12-04, 03:36:36
Author	

Project Properties

Title	Studies
-------	---------

Simulation Model 1:1

Study 1 - Static Stress

Study Properties

Study Type	Static Stress
Last Modification Date	2020-12-04, 03:30:25

Settings

General

Contact Tolerance	0.1 mm
Remove Rigid Body Modes	No

Damping

Mesh

Average Element Size (% of model size)	
Solids	10
Scale Mesh Size Per Part	No
Average Element Size (absolute value)	-
Element Order	Parabolic
Create Curved Mesh Elements	Yes
Max. Turn Angle on Curves (Deg.)	60
Max. Adjacent Mesh Size Ratio	1.5
Max. Aspect Ratio	10
Minimum Element Size (% of average size)	20

Adaptive Mesh Refinement

Number of Refinement Steps	0
Results Convergence Tolerance (%)	20
Portion of Elements to Refine (%)	10
Results for Baseline Accuracy	Von Mises Stress

Materials

Component	Material	Safety Factor
lower_body:1	ABS Plastic	Yield Strength

ABS Plastic

Density	1.06E-06 kg / mm ³
Young's Modulus	2240 MPa
Poisson's Ratio	0.38
Yield Strength	20 MPa
Ultimate Tensile Strength	29.6 MPa
Thermal Conductivity	1.6E-04 W / (mm C)
Thermal Expansion Coefficient	8.57E-05 / C
Specific Heat	1500 J / (kg C)

Contacts

Mesh

Type	Nodes	Elements
Solids	65549	39133

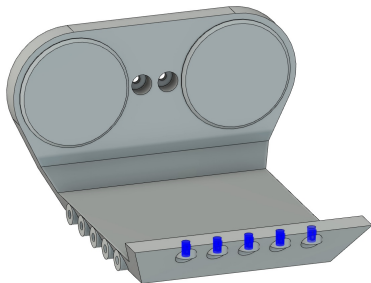
□ Load Case1

□ Constraints

□ Fixed1

Type	Fixed
Ux	Yes
Uy	Yes
Uz	Yes

□ Selected Entities

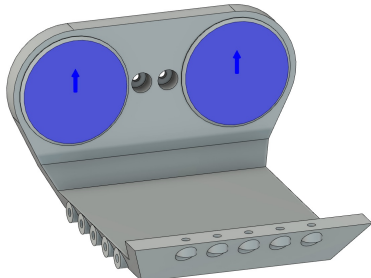


□ Loads

□ Force1

Type	Force
Magnitude	15 N
X Value	0 N
Y Value	1.887E-14 N
Z Value	15 N
X Angle	0 deg
Y Angle	-90 deg
Z Angle	0 deg
Force Per Entity	No

□ Selected Entities



□ Results

□ Result Summary

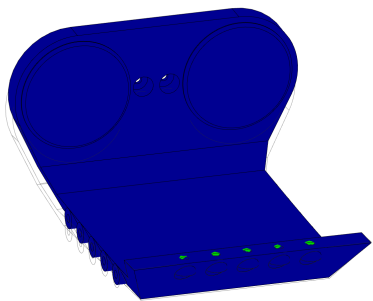
Name	Minimum	Maximum
Safety Factor		
Safety Factor (Per Body)	3.191	15
Stress		
Von Mises	6.09E-04 MPa	6.267 MPa
1st Principal	-4.128 MPa	8.883 MPa
3rd Principal	-10.96 MPa	3.919 MPa
Normal XX	-5.648 MPa	4.438 MPa
Normal YY	-9.367 MPa	8.123 MPa
Normal ZZ	-5.706 MPa	4.752 MPa
Shear XY	-1.75 MPa	2.064 MPa
Shear YZ	-2.632 MPa	1.135 MPa
Shear ZX	-1.273 MPa	1.086 MPa
Displacement		

Total	0 mm	1.142 mm
X	-0.004261 mm	0.00421 mm
Y	-0.09147 mm	0.6419 mm
Z	-0.03601 mm	0.9453 mm
Reaction Force		
Total	0 N	4.991 N
X	-1.931 N	2.137 N
Y	-4.898 N	4.498 N
Z	-2.431 N	2.114 N
Strain		
Equivalent	3.286E-07	0.004535
1st Principal	-6.674E-07	0.003636
3rd Principal	-0.004972	-2.89E-07
Normal XX	-7.954E-04	0.001075
Normal YY	-0.002255	0.002084
Normal ZZ	-8.057E-04	8.224E-04
Shear XY	-0.002157	0.002543
Shear YZ	-0.003244	0.001399
Shear ZX	-0.001568	0.001338

Safety Factor

Safety Factor (Per Body)

0  8



Stress

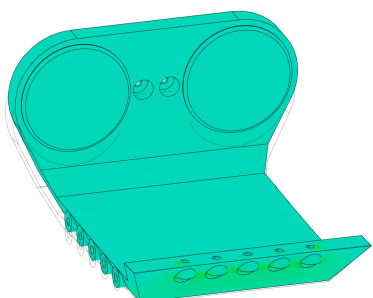
Von Mises

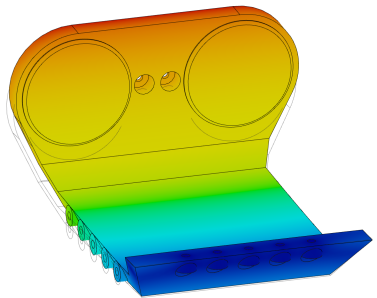
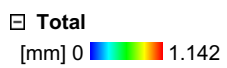
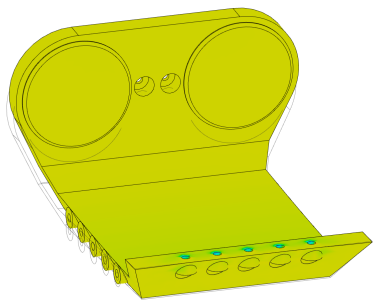
[MPa] 0.001  6.267



1st Principal

[MPa] -4.128  8.883





Chest Lower Link Analysis

Analyzed File	chest_2 v56
Version	Autodesk Fusion 360 (2.0.9313)
Creation Date	2020-12-04, 04:01:10
Author	

Project Properties

Title	Studies
-------	---------

Simulation Model 1:1

Study 1 - Static Stress

Study Properties

Study Type	Static Stress
Last Modification Date	2020-12-04, 03:52:24

Settings

General

Contact Tolerance	0.1 mm
Remove Rigid Body Modes	No

Damping

Mesh

Average Element Size (% of model size)	
Solids	10
Scale Mesh Size Per Part	No
Average Element Size (absolute value)	-
Element Order	Parabolic
Create Curved Mesh Elements	Yes
Max. Turn Angle on Curves (Deg.)	60
Max. Adjacent Mesh Size Ratio	1.5
Max. Aspect Ratio	10
Minimum Element Size (% of average size)	20

Adaptive Mesh Refinement

Number of Refinement Steps	0
Results Convergence Tolerance (%)	20
Portion of Elements to Refine (%)	10
Results for Baseline Accuracy	Von Mises Stress

Materials

Component	Material	Safety Factor
lower_link 1:1	ABS Plastic	Yield Strength

ABS Plastic

Density	1.06E-06 kg / mm ³
Young's Modulus	2240 MPa
Poisson's Ratio	0.38
Yield Strength	20 MPa
Ultimate Tensile Strength	29.6 MPa
Thermal Conductivity	1.6E-04 W / (mm C)
Thermal Expansion Coefficient	8.57E-05 / C
Specific Heat	1500 J / (kg C)

Contacts

Mesh

Type	Nodes	Elements
Solids	76731	42928

□ Load Case1

□ Constraints

□ Fixed1

Type	Fixed
Ux	Yes
Uy	Yes
Uz	Yes

□ Selected Entities



□ Loads

□ Force1

Type	Force
Magnitude	6.3 N
X Value	2.795E-10 N
Y Value	-6.437E-05 N
Z Value	6.3 N
X Angle	0 deg
Y Angle	0 deg
Z Angle	0 deg
Force Per Entity	No

□ Selected Entities



□ Results

□ Result Summary

Name	Minimum	Maximum
Safety Factor		
Safety Factor (Per Body)	3.02	15
Stress		
Von Mises	0.001161 MPa	6.623 MPa
1st Principal	-1.015 MPa	5.458 MPa
3rd Principal	-7.212 MPa	0.4252 MPa
Normal XX	-1.268 MPa	1.914 MPa
Normal YY	-5.71 MPa	4.814 MPa
Normal ZZ	-6.37 MPa	4.735 MPa
Shear XY	-1.72 MPa	1.618 MPa
Shear YZ	-2.282 MPa	2.678 MPa
Shear ZX	-2.261 MPa	1.861 MPa
Displacement		

Total	0 mm	46.23 mm
X	-1.147 mm	18.27 mm
Y	-0.02469 mm	39.76 mm
Z	-0.424 mm	18.61 mm
Reaction Force		
Total	0 N	14.02 N
X	-5.104 N	7.046 N
Y	-9.795 N	9.662 N
Z	-3.561 N	7.895 N
Strain		
Equivalent	8.935E-07	0.004435
1st Principal	6.142E-07	0.003595
3rd Principal	-0.004402	-6.301E-07
Normal XX	-8.146E-04	0.001165
Normal YY	-0.002479	0.00213
Normal ZZ	-0.002609	0.002029
Shear XY	-0.002119	0.001993
Shear YZ	-0.002812	0.0033
Shear ZX	-0.002786	0.002294

Safety Factor

Safety Factor (Per Body)

0  8



Stress

Von Mises

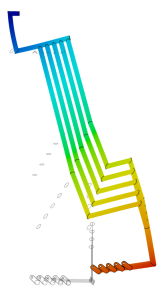
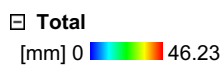
[MPa] 0.001  6.623



1st Principal

[MPa] -1.015  5.458





Chest Upper Body Analysis

Analyzed File	chest_2 v43
Version	Autodesk Fusion 360 (2.0.9313)
Creation Date	2020-12-04, 03:26:25
Author	

Project Properties

Title	Studies
-------	---------

Simulation Model 1:1

Study 1 - Static Stress

Study Properties

Study Type	Static Stress
Last Modification Date	2020-12-04, 03:21:03

Settings

General

Contact Tolerance	0.1 mm
Remove Rigid Body Modes	No

Damping

Mesh

Average Element Size (% of model size)	
Solids	10
Scale Mesh Size Per Part	No
Average Element Size (absolute value)	-
Element Order	Parabolic
Create Curved Mesh Elements	Yes
Max. Turn Angle on Curves (Deg.)	60
Max. Adjacent Mesh Size Ratio	1.5
Max. Aspect Ratio	10
Minimum Element Size (% of average size)	20

Adaptive Mesh Refinement

Number of Refinement Steps	0
Results Convergence Tolerance (%)	20
Portion of Elements to Refine (%)	10
Results for Baseline Accuracy	Von Mises Stress

Materials

Component	Material	Safety Factor
upper_body:1	ABS Plastic	Yield Strength

ABS Plastic

Density	1.06E-06 kg / mm ³
Young's Modulus	2240 MPa
Poisson's Ratio	0.38
Yield Strength	20 MPa
Ultimate Tensile Strength	29.6 MPa
Thermal Conductivity	1.6E-04 W / (mm C)
Thermal Expansion Coefficient	8.57E-05 / C
Specific Heat	1500 J / (kg C)

Contacts

Mesh

Type	Nodes	Elements
Solids	95190	61326

□ Load Case1

□ Constraints

□ Fixed1

Type	Fixed
Ux	Yes
Uy	Yes
Uz	Yes

□ Selected Entities



□ Loads

□ Force1

Type	Force
Magnitude	85 N
X Value	0 N
Y Value	-1.781E-07 N
Z Value	-85 N
X Angle	-180 deg
Y Angle	0 deg
Z Angle	0 deg
Force Per Entity	No

□ Selected Entities



□ Results

□ Result Summary

Name	Minimum	Maximum
Safety Factor		
Safety Factor (Per Body)	3.045	15
Stress		
Von Mises	0.001736 MPa	6.567 MPa
1st Principal	-2.879 MPa	8.387 MPa
3rd Principal	-8.879 MPa	1.886 MPa
Normal XX	-5.038 MPa	4.524 MPa
Normal YY	-7.341 MPa	6.315 MPa
Normal ZZ	-5.038 MPa	4.026 MPa
Shear XY	-1.81 MPa	1.777 MPa
Shear YZ	-1.933 MPa	3.042 MPa
Shear ZX	-1.442 MPa	1.373 MPa
Displacement		

Total	0 mm	31.53 mm
X	-0.02738 mm	0.02839 mm
Y	-29.1 mm	0.04036 mm
Z	-12.15 mm	0.5741 mm
Reaction Force		
Total	0 N	45.03 N
X	-14.61 N	13.09 N
Y	-8.872 N	38.08 N
Z	-23.81 N	21.09 N
Strain		
Equivalent	1.04E-06	0.004628
1st Principal	8.365E-07	0.004849
3rd Principal	-0.004383	9.892E-07
Normal XX	-0.001	0.001062
Normal YY	-0.001971	0.0022
Normal ZZ	-0.002393	0.001697
Shear XY	-0.00223	0.00219
Shear YZ	-0.002381	0.003748
Shear ZX	-0.001776	0.001692

Safety Factor

Safety Factor (Per Body)

0  8



Stress

Von Mises

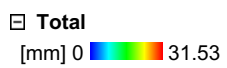
[MPa] 0.002  6.567



1st Principal

[MPa] -2.879  8.387





Chest Upper Link Analysis

Analyzed File	chest_2 v51
Version	Autodesk Fusion 360 (2.0.9313)
Creation Date	2020-12-04, 03:48:31
Author	

Project Properties

Title	Studies
-------	---------

Simulation Model 1:1

Study 1 - Static Stress

Study Properties

Study Type	Static Stress
Last Modification Date	2020-12-04, 03:40:40

Settings

General

Contact Tolerance	0.1 mm
Remove Rigid Body Modes	No

Damping

Mesh

Average Element Size (% of model size)	
Solids	10
Scale Mesh Size Per Part	No
Average Element Size (absolute value)	-
Element Order	Parabolic
Create Curved Mesh Elements	Yes
Max. Turn Angle on Curves (Deg.)	60
Max. Adjacent Mesh Size Ratio	1.5
Max. Aspect Ratio	10
Minimum Element Size (% of average size)	20

Adaptive Mesh Refinement

Number of Refinement Steps	0
Results Convergence Tolerance (%)	20
Portion of Elements to Refine (%)	10
Results for Baseline Accuracy	Von Mises Stress

Materials

Component	Material	Safety Factor
upper_link:1	ABS Plastic	Yield Strength

ABS Plastic

Density	1.06E-06 kg / mm ³
Young's Modulus	2240 MPa
Poisson's Ratio	0.38
Yield Strength	20 MPa
Ultimate Tensile Strength	29.6 MPa
Thermal Conductivity	1.6E-04 W / (mm C)
Thermal Expansion Coefficient	8.57E-05 / C
Specific Heat	1500 J / (kg C)

Contacts

Mesh

Type	Nodes	Elements
Solids	92567	51960

□ Load Case1

□ Constraints

□ Fixed1

Type	Fixed
Ux	Yes
Uy	Yes
Uz	Yes

□ Selected Entities

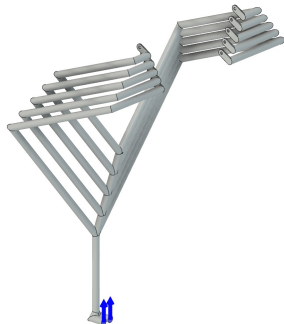


□ Loads

□ Force1

Type	Force
Magnitude	7 N
X Value	0 N
Y Value	8.974E-14 N
Z Value	7 N
X Angle	0 deg
Y Angle	-90 deg
Z Angle	0 deg
Force Per Entity	No

□ Selected Entities



□ Results

□ Result Summary

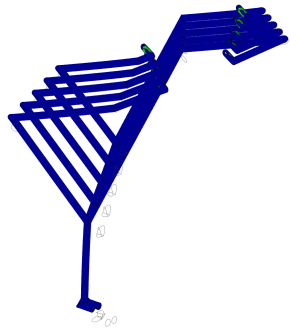
Name	Minimum	Maximum
Safety Factor		
Safety Factor (Per Body)	3.239	15
Stress		
Von Mises	0.001488 MPa	6.174 MPa
1st Principal	-1.898 MPa	7.522 MPa
3rd Principal	-6.207 MPa	1.901 MPa
Normal XX	-2.662 MPa	3.346 MPa
Normal YY	-5.067 MPa	7.497 MPa
Normal ZZ	-3.679 MPa	3.654 MPa
Shear XY	-1.174 MPa	1.032 MPa
Shear YZ	-2.524 MPa	2.924 MPa
Shear ZX	-1.006 MPa	1.096 MPa
Displacement		

Total	0 mm	9.217 mm
X	-0.5884 mm	0.5935 mm
Y	-8.321 mm	0.171 mm
Z	-0.1112 mm	4.044 mm
Reaction Force		
Total	0 N	5.121 N
X	-3.568 N	3.546 N
Y	-3.685 N	4.187 N
Z	-3.516 N	3.755 N
Strain		
Equivalent	9.04E-07	0.004231
1st Principal	6.338E-07	0.004063
3rd Principal	-0.004086	-7.071E-07
Normal XX	-0.001094	0.001123
Normal YY	-0.002056	0.002514
Normal ZZ	-0.001667	0.001056
Shear XY	-0.001447	0.001272
Shear YZ	-0.00311	0.003603
Shear ZX	-0.001239	0.001351

Safety Factor

Safety Factor (Per Body)

0  8



Stress

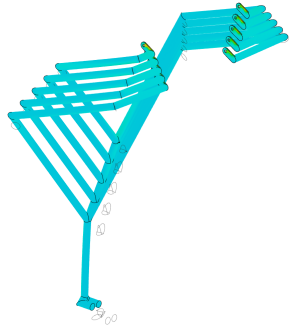
Von Mises

[MPa] 0.001  6.174



1st Principal

[MPa] -1.898  7.522



3rd Principal

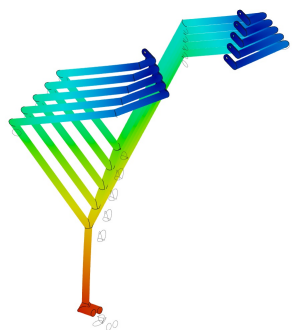
[MPa] -6.207  1.901



Displacement

Total

[mm] 0  9.217



Hand Lower Arm Analysis

Analyzed File	hand_3 v46
Version	Autodesk Fusion 360 (2.0.9313)
Creation Date	2020-12-04, 02:46:00
Author	

Project Properties

Title	Studies
-------	---------

Simulation Model 1:1

Study 1 - Static Stress

Study Properties

Study Type	Static Stress
Last Modification Date	2020-12-04, 02:31:15

Settings

General

Contact Tolerance	0.1 mm
Remove Rigid Body Modes	No

Damping

Mesh

Average Element Size (% of model size)	
Solids	10
Scale Mesh Size Per Part	No
Average Element Size (absolute value)	-
Element Order	Parabolic
Create Curved Mesh Elements	Yes
Max. Turn Angle on Curves (Deg.)	60
Max. Adjacent Mesh Size Ratio	1.5
Max. Aspect Ratio	10
Minimum Element Size (% of average size)	20

Adaptive Mesh Refinement

Number of Refinement Steps	0
Results Convergence Tolerance (%)	20
Portion of Elements to Refine (%)	10
Results for Baseline Accuracy	Von Mises Stress

Materials

Component	Material	Safety Factor
lower_arm:1	ABS Plastic	Yield Strength

ABS Plastic

Density	1.06E-06 kg / mm ³
Young's Modulus	2240 MPa
Poisson's Ratio	0.38
Yield Strength	20 MPa
Ultimate Tensile Strength	29.6 MPa
Thermal Conductivity	1.6E-04 W / (mm C)
Thermal Expansion Coefficient	8.57E-05 / C
Specific Heat	1500 J / (kg C)

Contacts

Mesh

Type	Nodes	Elements
Solids	9769	5654

□ Load Case1

□ Constraints

□ Fixed1

Type	Fixed
Ux	Yes
Uy	Yes
Uz	Yes

□ Selected Entities



□ Loads

□ Force1

Type	Force
Magnitude	414 N
X Value	-5.318 N
Y Value	-354 N
Z Value	-214.6 N
X Angle	-180 deg
Y Angle	0 deg
Z Angle	0 deg
Force Per Entity	No

□ Selected Entities



□ Results

□ Result Summary

Name	Minimum	Maximum
Safety Factor		
Safety Factor (Per Body)	3.004	15
Stress		
Von Mises	0.01215 MPa	6.657 MPa
1st Principal	-2.133 MPa	10.57 MPa
3rd Principal	-7.502 MPa	5.131 MPa
Normal XX	-7.499 MPa	5.893 MPa
Normal YY	-4.254 MPa	8.788 MPa
Normal ZZ	-3.747 MPa	7.04 MPa
Shear XY	-1.772 MPa	1.594 MPa
Shear YZ	-2.577 MPa	3.078 MPa
Shear ZX	-0.9584 MPa	1.167 MPa
Displacement		

Total	0 mm	0.8349 mm
X	-0.657 mm	0.004623 mm
Y	-0.4382 mm	0.03031 mm
Z	-0.2717 mm	0.01285 mm
Reaction Force		
Total	0 N	6.561 N
X	-2.043 N	2.473 N
Y	-1.519 N	5.393 N
Z	-1.131 N	3.736 N
Strain		
Equivalent	7.206E-06	0.004533
1st Principal	5.754E-06	0.004648
3rd Principal	-0.003669	-4.121E-06
Normal XX	-0.002826	0.002159
Normal YY	-0.001722	0.002296
Normal ZZ	-0.002153	0.001949
Shear XY	-0.002183	0.001964
Shear YZ	-0.003176	0.003793
Shear ZX	-0.001181	0.001438

Safety Factor

Safety Factor (Per Body)

0  8



Stress

Von Mises

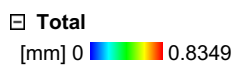
[MPa] 0.012  6.657



1st Principal

[MPa] -2.13  10.57





Hand Upper Arm Analysis

Analyzed File	hand_3 v36
Version	Autodesk Fusion 360 (2.0.9313)
Creation Date	2020-12-04, 02:26:24
Author	

Project Properties

Title	Studies
-------	---------

Simulation Model 1:1

Study 1 - Static Stress

Study Properties

Study Type	Static Stress
Last Modification Date	2020-12-04, 02:15:46

Settings

General

Contact Tolerance	0.1 mm
Remove Rigid Body Modes	No

Damping

Mesh

Average Element Size (% of model size)	
Solids	10
Scale Mesh Size Per Part	No
Average Element Size (absolute value)	-
Element Order	Parabolic
Create Curved Mesh Elements	Yes
Max. Turn Angle on Curves (Deg.)	60
Max. Adjacent Mesh Size Ratio	1.5
Max. Aspect Ratio	10
Minimum Element Size (% of average size)	20

Adaptive Mesh Refinement

Number of Refinement Steps	0
Results Convergence Tolerance (%)	20
Portion of Elements to Refine (%)	10
Results for Baseline Accuracy	Von Mises Stress

Materials

Component	Material	Safety Factor
upper_arm:1	ABS Plastic	Yield Strength

ABS Plastic

Density	1.06E-06 kg / mm ³
Young's Modulus	2240 MPa
Poisson's Ratio	0.38
Yield Strength	20 MPa
Ultimate Tensile Strength	29.6 MPa
Thermal Conductivity	1.6E-04 W / (mm C)
Thermal Expansion Coefficient	8.57E-05 / C
Specific Heat	1500 J / (kg C)

Contacts

Mesh

Type	Nodes	Elements
Solids	17543	10190

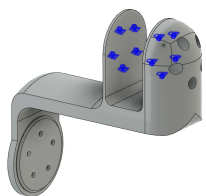
□ Load Case1

□ Constraints

□ Fixed1

Type	Fixed
Ux	Yes
Uy	Yes
Uz	Yes

□ Selected Entities

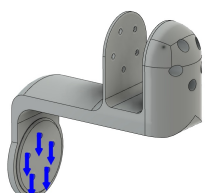


□ Loads

□ Force1

Type	Force
Magnitude	49 N
X Value	-4.14E-04 N
Y Value	-0.0486 N
Z Value	-49 N
X Angle	160 deg
Y Angle	0 deg
Z Angle	0 deg
Force Per Entity	No

□ Selected Entities



□ Results

□ Result Summary

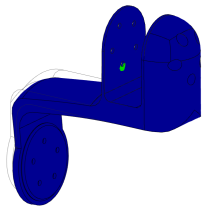
Name	Minimum	Maximum
Safety Factor		
Safety Factor (Per Body)	3.011	15
Stress		
Von Mises	0.001116 MPa	6.642 MPa
1st Principal	-2.105 MPa	11.39 MPa
3rd Principal	-4.725 MPa	4.216 MPa
Normal XX	-3.775 MPa	5.753 MPa
Normal YY	-2.588 MPa	4.445 MPa
Normal ZZ	-4.242 MPa	11.21 MPa
Shear XY	-0.7131 MPa	0.7795 MPa
Shear YZ	-1.116 MPa	1.014 MPa
Shear ZX	-2.256 MPa	2.146 MPa
Displacement		

Total	0 mm	0.5873 mm
X	-0.006626 mm	0.005865 mm
Y	-0.4139 mm	0.04682 mm
Z	-0.4224 mm	0.006261 mm
Reaction Force		
Total	0 N	6.708 N
X	-2.086 N	2.052 N
Y	-3.214 N	3.251 N
Z	-2.21 N	6.173 N
Strain		
Equivalent	6.034E-07	0.003767
1st Principal	4.549E-07	0.004184
3rd Principal	-0.00247	-5.81E-07
Normal XX	-0.001225	6.941E-04
Normal YY	-0.001425	0.001086
Normal ZZ	-0.001084	0.00331
Shear XY	-8.787E-04	9.604E-04
Shear YZ	-0.001375	0.001249
Shear ZX	-0.00278	0.002644

Safety Factor

Safety Factor (Per Body)

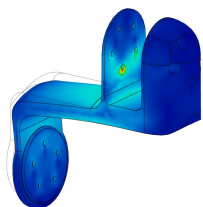
0  8



Stress

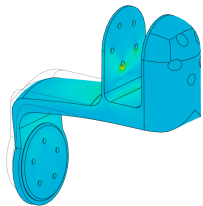
Von Mises

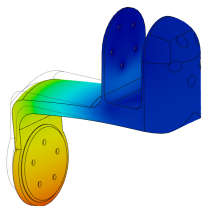
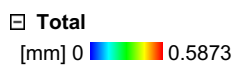
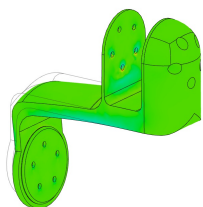
[MPa] 0.001  6.642



1st Principal

[MPa] -2.1  11.39





Leg Lower Analysis

Analyzed File	leg_4 v22
Version	Autodesk Fusion 360 (2.0.9313)
Creation Date	2020-12-04, 03:11:37
Author	

Project Properties

Title	Studies
-------	---------

Simulation Model 1:1

Study 1 - Static Stress

Study Properties

Study Type	Static Stress
Last Modification Date	2020-12-04, 03:04:36

Settings

General

Contact Tolerance	0.1 mm
Remove Rigid Body Modes	No

Damping

Mesh

Average Element Size (% of model size)	
Solids	10
Scale Mesh Size Per Part	No
Average Element Size (absolute value)	-
Element Order	Parabolic
Create Curved Mesh Elements	Yes
Max. Turn Angle on Curves (Deg.)	60
Max. Adjacent Mesh Size Ratio	1.5
Max. Aspect Ratio	10
Minimum Element Size (% of average size)	20

Adaptive Mesh Refinement

Number of Refinement Steps	0
Results Convergence Tolerance (%)	20
Portion of Elements to Refine (%)	10
Results for Baseline Accuracy	Von Mises Stress

Materials

Component	Material	Safety Factor
lower_leg:1	ABS Plastic	Yield Strength

ABS Plastic

Density	1.06E-06 kg / mm ³
Young's Modulus	2240 MPa
Poisson's Ratio	0.38
Yield Strength	20 MPa
Ultimate Tensile Strength	29.6 MPa
Thermal Conductivity	1.6E-04 W / (mm C)
Thermal Expansion Coefficient	8.57E-05 / C
Specific Heat	1500 J / (kg C)

Contacts

Mesh

Type	Nodes	Elements
Solids	11809	6822

□ Load Case1

□ Constraints

□ Fixed1

Type	Fixed
Ux	Yes
Uy	Yes
Uz	Yes

□ Selected Entities



□ Loads

□ Force1

Type	Force
Magnitude	55 N
X Value	0 N
Y Value	21.6 N
Z Value	50.58 N
X Angle	0 deg
Y Angle	45 deg
Z Angle	0 deg
Force Per Entity	No

□ Selected Entities



□ Results

□ Result Summary

Name	Minimum	Maximum
Safety Factor		
Safety Factor (Per Body)	3.048	15
Stress		
Von Mises	0.0175 MPa	6.562 MPa
1st Principal	-3.876 MPa	8.894 MPa
3rd Principal	-7.864 MPa	3.51 MPa
Normal XX	-4.368 MPa	4.556 MPa
Normal YY	-4.29 MPa	4.896 MPa
Normal ZZ	-7.589 MPa	7.484 MPa
Shear XY	-0.8192 MPa	0.8281 MPa
Shear YZ	-2.631 MPa	3.718 MPa
Shear ZX	-0.92 MPa	1.049 MPa
Displacement		

Total	0 mm	0.4567 mm
X	-0.005408 mm	0.005341 mm
Y	-0.004398 mm	0.4259 mm
Z	-0.0232 mm	0.204 mm
Reaction Force		
Total	0 N	5.976 N
X	-2.105 N	2.073 N
Y	-4.197 N	2.773 N
Z	-5.588 N	5.535 N
Strain		
Equivalent	1.074E-05	0.005388
1st Principal	7.006E-06	0.004667
3rd Principal	-0.004664	-1.098E-05
Normal XX	-9.139E-04	0.001042
Normal YY	-0.0017	0.001745
Normal ZZ	-0.002372	0.002541
Shear XY	-0.001009	0.00102
Shear YZ	-0.003241	0.004581
Shear ZX	-0.001134	0.001293

Safety Factor

Safety Factor (Per Body)

0  8



Stress

Von Mises

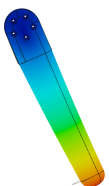
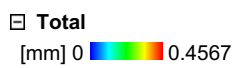
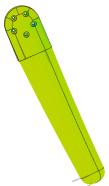
[MPa] 0.017  6.562



1st Principal

[MPa] -3.876  8.894





Leg Upper Analysis

Analyzed File	leg_4 v17
Version	Autodesk Fusion 360 (2.0.9313)
Creation Date	2020-12-04, 02:59:44
Author	

Project Properties

Title	Studies
-------	---------

Simulation Model 1:1

Study 1 - Static Stress

Study Properties

Study Type	Static Stress
Last Modification Date	2020-12-04, 02:49:20

Settings

General

Contact Tolerance	0.1 mm
Remove Rigid Body Modes	No

Damping

Mesh

Average Element Size (% of model size)	
Solids	10
Scale Mesh Size Per Part	No
Average Element Size (absolute value)	-
Element Order	Parabolic
Create Curved Mesh Elements	Yes
Max. Turn Angle on Curves (Deg.)	60
Max. Adjacent Mesh Size Ratio	1.5
Max. Aspect Ratio	10
Minimum Element Size (% of average size)	20

Adaptive Mesh Refinement

Number of Refinement Steps	0
Results Convergence Tolerance (%)	20
Portion of Elements to Refine (%)	10
Results for Baseline Accuracy	Von Mises Stress

Materials

Component	Material	Safety Factor
upper_leg:1	ABS Plastic	Yield Strength

ABS Plastic

Density	1.06E-06 kg / mm ³
Young's Modulus	2240 MPa
Poisson's Ratio	0.38
Yield Strength	20 MPa
Ultimate Tensile Strength	29.6 MPa
Thermal Conductivity	1.6E-04 W / (mm C)
Thermal Expansion Coefficient	8.57E-05 / C
Specific Heat	1500 J / (kg C)

Contacts

Mesh

Type	Nodes	Elements
Solids	9660	5662

□ Load Case1

□ Constraints

□ Fixed1

Type	Fixed
Ux	Yes
Uy	Yes
Uz	Yes

□ Selected Entities



□ Loads

□ Force1

Type	Force
Magnitude	357 N
X Value	-3.526E-29 N
Y Value	-4.349E-29 N
Z Value	357 N
Force Per Entity	No

□ Selected Entities



□ Results

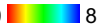
□ Result Summary

Name	Minimum	Maximum
Safety Factor		
Safety Factor (Per Body)	3.005	15
Stress		
Von Mises	0.005511 MPa	6.655 MPa
1st Principal	-5.567 MPa	8.976 MPa
3rd Principal	-12.66 MPa	3.764 MPa
Normal XX	-6.558 MPa	5.527 MPa
Normal YY	-6.826 MPa	4.829 MPa
Normal ZZ	-11.4 MPa	7.702 MPa
Shear XY	-2.02 MPa	1.982 MPa
Shear YZ	-1.803 MPa	2.693 MPa
Shear ZX	-2.858 MPa	2.67 MPa
Displacement		
Total	0 mm	0.05927 mm
X	-0.002379 mm	0.002386 mm
Y	-0.0511 mm	0.0121 mm

Z	-9.265E-04 mm	0.03003 mm
Reaction Force		
Total	0 N	5.507 N
X	-2.581 N	2.409 N
Y	-2.3 N	2.862 N
Z	-5.252 N	3.159 N
Strain		
Equivalent	2.982E-06	0.004985
1st Principal	2.521E-06	0.004258
3rd Principal	-0.005295	-6.064E-07
Normal XX	-0.00129	0.001544
Normal YY	-5.565E-04	0.001154
Normal ZZ	-0.002821	0.001832
Shear XY	-0.00249	0.002443
Shear YZ	-0.002222	0.003319
Shear ZX	-0.003521	0.00329

Safety Factor

Safety Factor (Per Body)

0  8



Stress

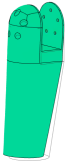
Von Mises

[MPa] 0.006  6.655



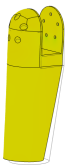
1st Principal

[MPa] -5.567  8.976



3rd Principal

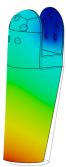
[MPa] -12.66  3.76



Displacement

Total

[mm] 0  0.05927



6. ADAPTIVE CMAC BASED DYNAMIC BALANCING AND ZMP COMPENSATION DESIGN

6.1 CMAC

CMAC based adaptive control system:

- Self-learning control parameter
- Simple computation
- Better control performance

6.2 RCMAC

Input Space:

$$\mathbf{p} = [p_1, p_2, \dots, p_{n_a}]^T \in \Re^{n_a}$$

Association Memory Space:

$$\mu_{ik} = \exp \left[\frac{-(p_i - c_{ik})^2}{\sigma_{ik}^2} \right]$$

Recurrent Unit:

$$p_{rik}(t) = p_i(t) + r_{ik}\mu_{ik}(t - T)$$

Receptive-Filed Space:

$$\phi_k(\mathbf{p}, \mathbf{c}_k, \mathbf{v}_k, \mathbf{r}_k) = \prod_{i=1}^{n_a} \mu_{ik} = \exp \left[\sum_{i=1}^{n_g} \frac{-(p_{rik} - c_{ik})^2}{\sigma_{ik}^2} \right]$$

Output Space:

$$o_p = \mathbf{w}_p^T \Phi = \sum_{k=1}^{n_d} w_{kp} \phi_k$$

6.3 ADAPTIVE CMAC CONTROL SYSTEM

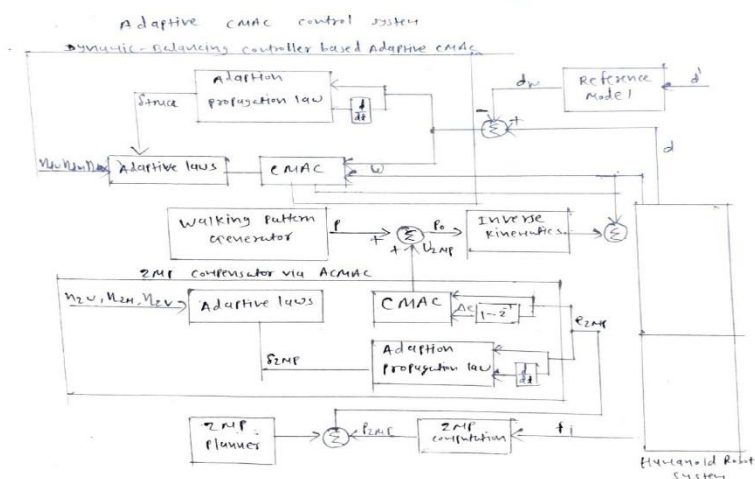


Fig 30: ACMAC control system [9]

6.4 ACMAC BASED DYNAMIC BALANCING

The tracking error of dynamic-balancing controller is defined as
 $e_{\text{truck}} = d_m - d$

And the output of the ACMAC-based dynamic-balancing is U_{Hip} .

The total desired is defined as

$$\tau = \tau_o + U_{\text{Hip}}$$

The tracking error of dynamic-balancing controller is defined as

$$e_{ZMP} = d_{ZMP} - p_{ZMP}$$

And the output of the ACMAC-based dynamic-balancing is U_{ZMP} .

6.5 ACMAC BASED ZMP COMPENSATOR

The total desired hip trajectories is defined as

$$P_o = P + U_{ZMP}$$

6.6 ONLINE LEARNING ALGORITHM

The energy function, E, is defined as $E = \frac{1}{2}(d_m - d)^2 = \frac{1}{2}e_m^2$ with the energy function, the error term to be propagated is given by

$$\delta_{ZMP} = -\frac{\partial E}{\partial U_{ZMP}} = -\frac{\partial E}{\partial e_m} \frac{\partial e_m}{\partial d} \frac{\partial d}{\partial U_{ZUP}}$$

, based on backpropagation method can be derived as

$$\begin{aligned}\Delta w_z &= -\eta_{zw} \frac{\partial E}{\partial w_z} = -\eta_{zw} \frac{\partial E}{\partial U_{ZMP}} \frac{\partial U_{ZMP}}{\partial w_z} = -\eta_{zw} \delta_{ZMP} \phi_k \\ \Delta m_{ik} &= -\eta_{zm} \frac{\partial E}{\partial U_{ZMP}} \frac{\partial U_{ZMP}}{\partial \phi_k} \frac{\partial \phi_k}{\partial \mu_{ik}} \frac{\partial \mu_{ik}}{\partial m_{ik}} = -\eta_{zm} \delta_{ZMP} w_z \phi_k \frac{2(p_{rik} - m_{ik})}{v_{ik}^2} \\ \Delta v_{ik} &= -\eta_{zv} \frac{\partial E}{\partial U_{ZMP}} \frac{\partial U_{ZMP}}{\partial \phi_k} \frac{\partial \phi_k}{\partial \mu_{ik}} \frac{\partial \mu_{ik}}{\partial v_{ik}} = -\eta_{zv} \delta_{ZMP} w_z \phi_k \frac{2(p_{rik} - m_{ik})^2}{v_{ik}^3} \\ \Delta r_{ik} &= -\eta_{zr} \frac{\partial E}{\partial U_{ZMP}} \frac{\partial U_{ZMP}}{\partial \phi_k} \frac{\partial \phi_k}{\partial \mu_{ik}} \frac{\partial \mu_{ik}}{\partial r_{ik}} = -\eta_{zr} \delta_{ZMP} w_z \phi_k \frac{2(m_{ik} - p_{rik})}{v_{ik}^2} \mu_{ik}(t - T)\end{aligned}$$

$\partial d / \partial U_{ZMP}$ cannot be computed if the plant model is unknown, an adaptation propagation law is given by

$$\delta_{ZMP} \cong (\dot{d}_m - \dot{d}) + (d_m - d) = \Delta e_m + e_m$$

7. MECHANICS OF ROBOT

Normal robot containing solid blocks, rigid transformations and joint blocks.

7.1 MECHANISM

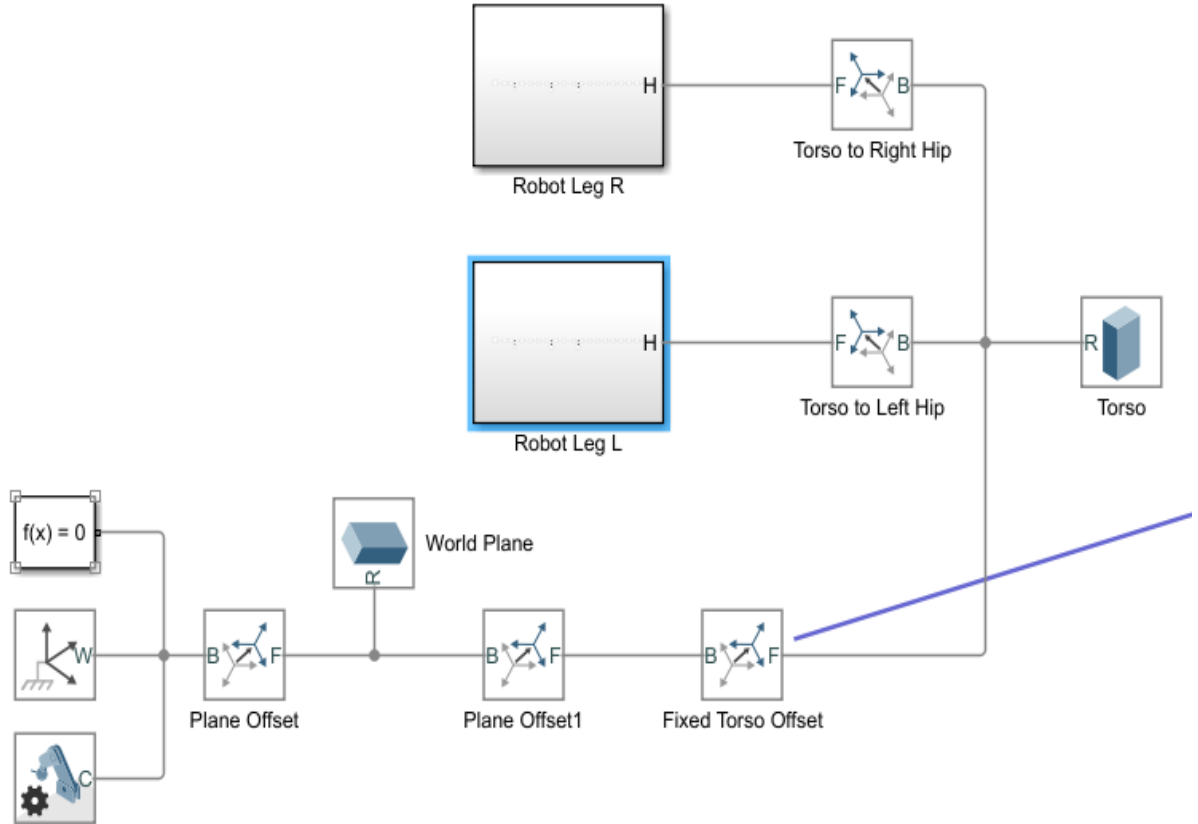


Fig 31: Mechanism of Robot

Setting conditions such as changing pitch value of hip joint to half and decreasing damping to $1/10^{\text{th}}$. Initializing conditions such as stiffness, damping, length, width and height, etc.

7.2 LEG MECHANISM

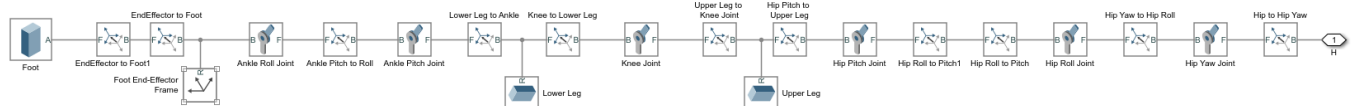


Fig 32: Leg Mechanism of Robot

8. LIPM

8.1 ASSUMPTIONS

Linear Inverted Pendulum Model is a simple and powerful model:

- Robot has constant height while walking
- Angular momentum around CoM is very small

8.2 FINDING INITIAL CONDITIONS

Finding initial conditions and time to create symmetric piece of trajectory, will be sufficient as we are simulating our model to walk in a straight line. Mirroring the same for the other leg.

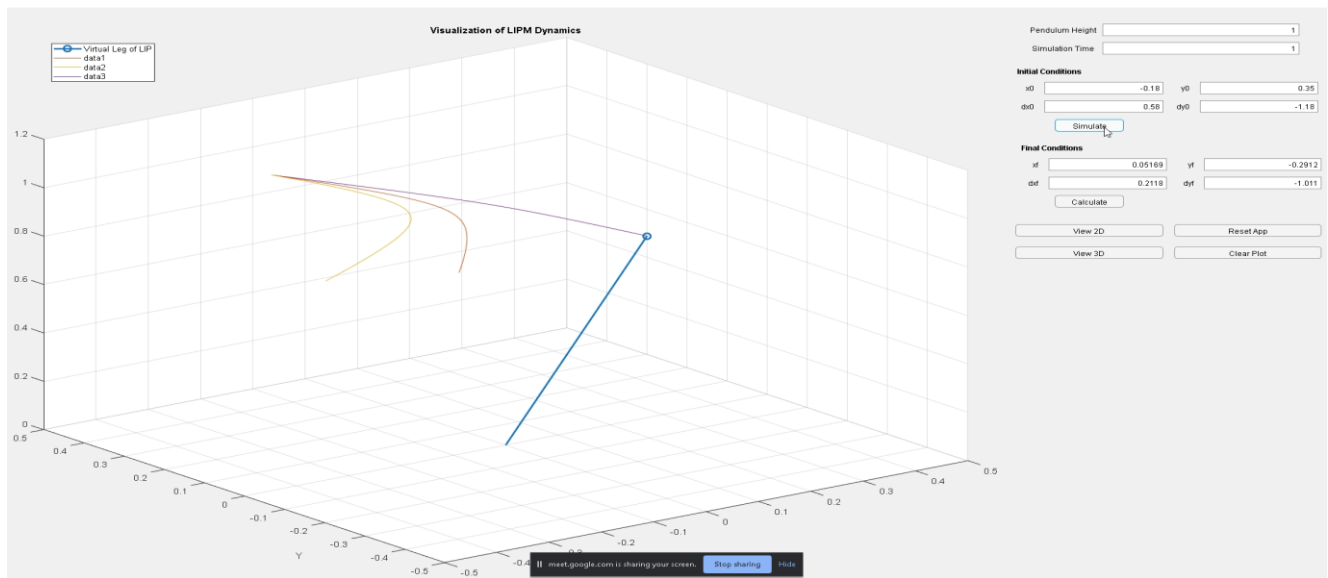


Fig 33: LIPM Symmetry 1

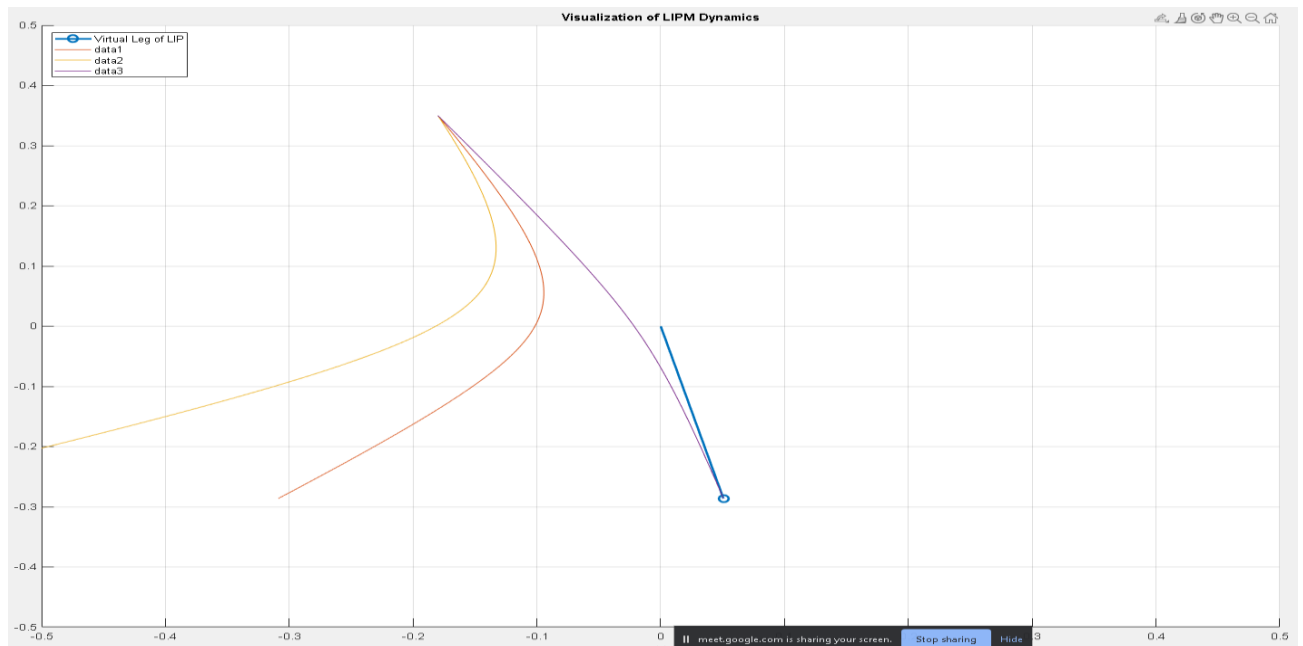


Fig 34: LIPM Symmetry 2

8.3 SETTING PARAMETERS

Setting parameters like height, swing height, step length, velocity, etc.

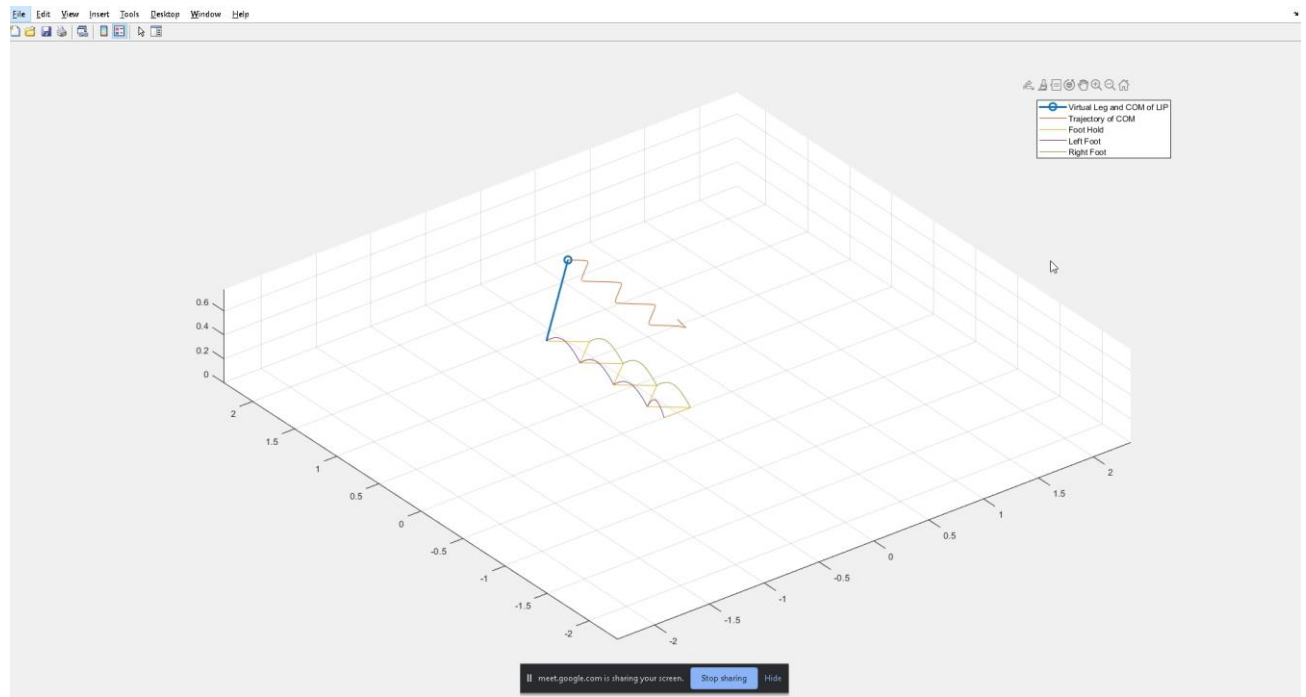


Fig 35: CoM Trajectory

8.4 FINDING JOINT ANGLES

Finding joint angles from feet trajectories using inverse kinematics. Inverse rotations for joint angles are done through analytical solution.

```
dhparams = [L1      0       -L2      0;
            0       -pi/2    0       0;
            0       -pi/2    0       0;
            L3      0       0       0;
            L4      0       0       0;
            0       pi/2    0       0;
            0       0       L5     0];
```

Fig 36: DH Parameters

```

%% 2) Get inverse rotation matrix (in this case, a transpose)
Rp = R';
n = Rp(:, 1);
s = Rp(:, 2);
a = Rp(:, 3);
p = -Rp*p;

%% 3) Compute nalytic solution from the paper
cos4 = ((p(1)+L5)^2 + p(2)^2 + p(3)^2 - L3^2 - L4^2) / (2*L3*L4);
temp = 1 - cos4^2;
if temp < 0
    temp = 0;
    disp('Warning: Unable to reach desired end-effector position/orientation');
end

th4 = atan2(sqrt(temp), cos4);
% NOTE: you can put -sqrt(temp) to change direction of knee bending
temp = (p(1)+L5)^2+p(2)^2;
if temp < 0
    temp = 0;
    disp('Warning: Unable to reach desired end-effector position/orientation');
end
th5 = atan2(-p(3), sqrt(temp))-atan2(sin(th4)*L3, cos(th4)*L3+L4);
th6 = atan2(p(2), -p(1)-L5);
temp = 1-(sin(th6)*a(1)+cos(th6)*a(2))^2;
if temp < 0
    temp = 0;
    disp('Warning: Unable to reach desired end-effector position/orientation');
end
th2 = atan2(-sqrt(temp), sin(th6)*a(1)+cos(th6)*a(2));
th2 = th2 + pi/2; % pi/2 offset
th1 = atan2(-sin(th6)*s(1)-cos(th6)*s(2), -sin(th6)*n(1)-cos(th6)*n(2));

```

Fig 37: Analytical Computation

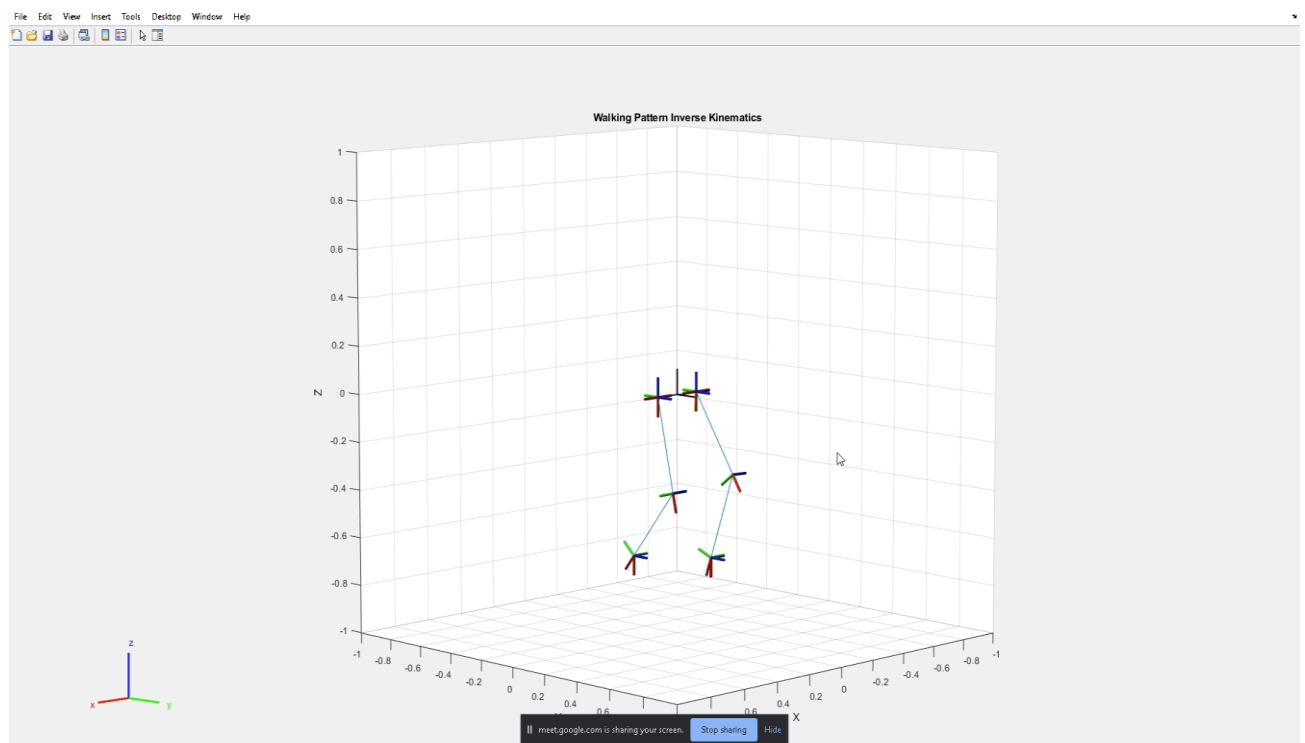


Fig 38: Walking Trajectory

9. SIMULATION

Joint angles of legs are feed as input in our model. Simulation is done through simplified motion approach

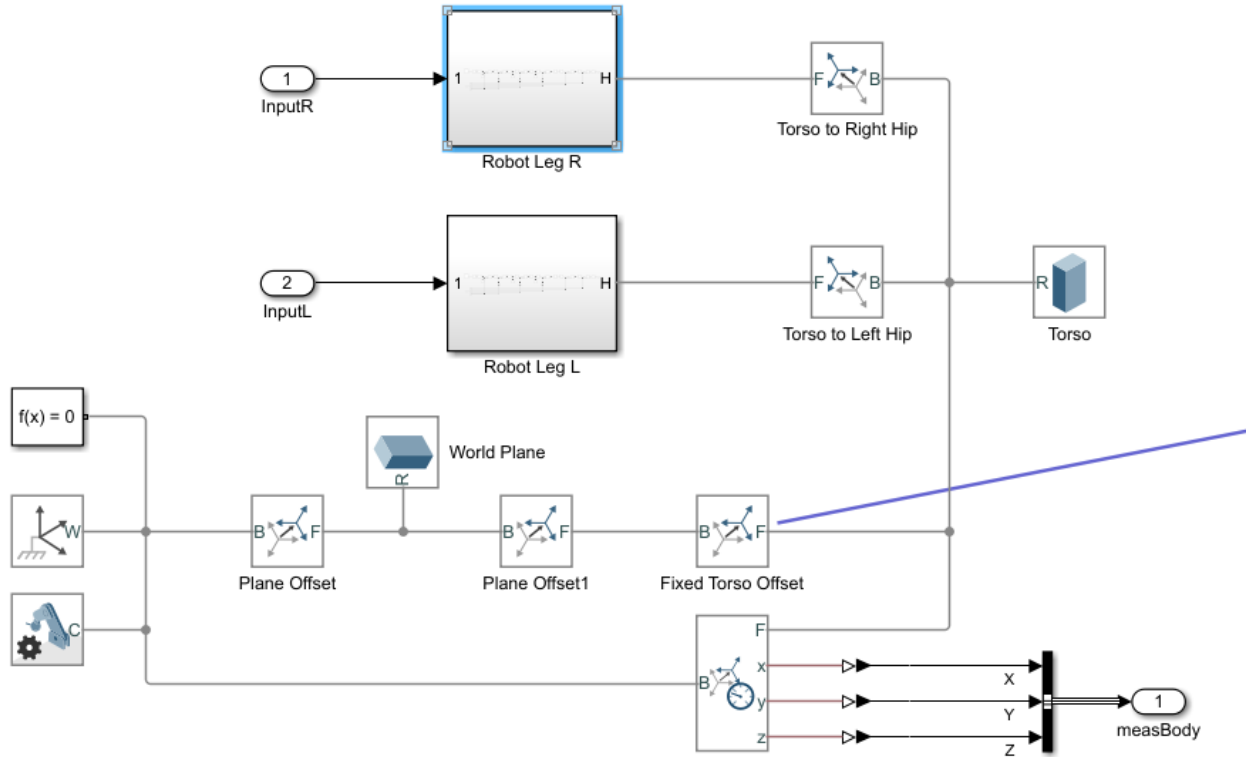


Fig 39: Input Joint Angles

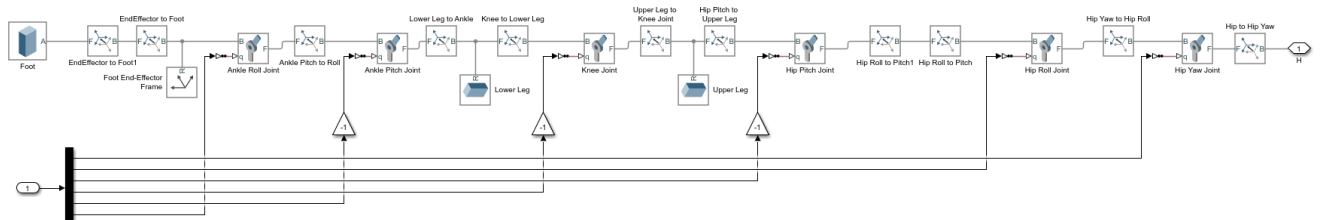


Fig 40: Input Joint Angles 2

10. GRAPHS

We used motion actuation for actuating robot joints because it is easier and faster to simulate and does not offer much difference from force / torque actuation approach.

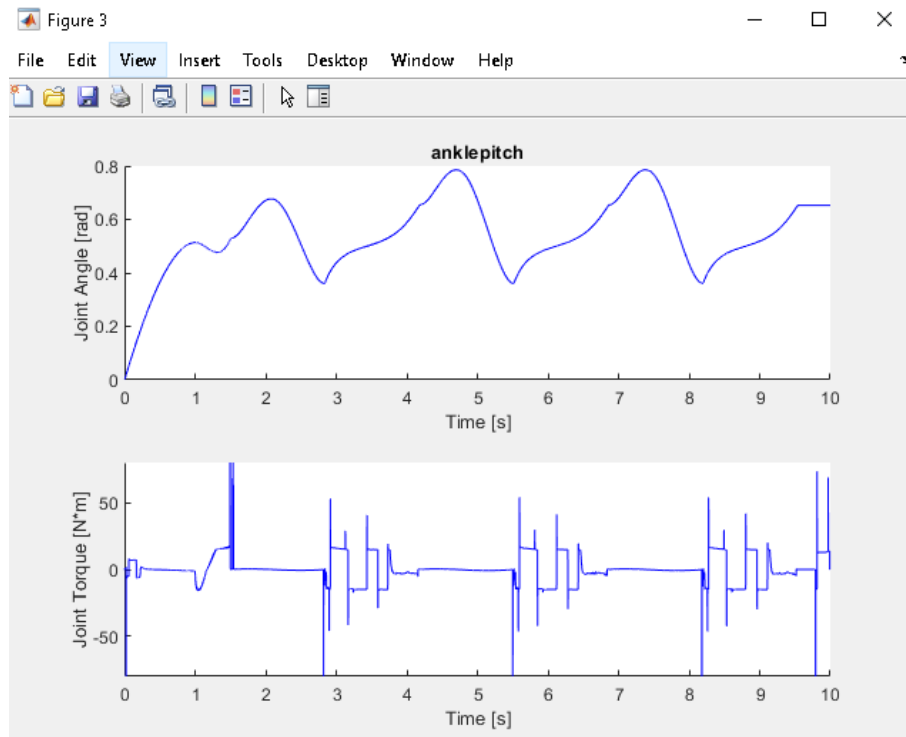


Fig 41: Ankle Pitch

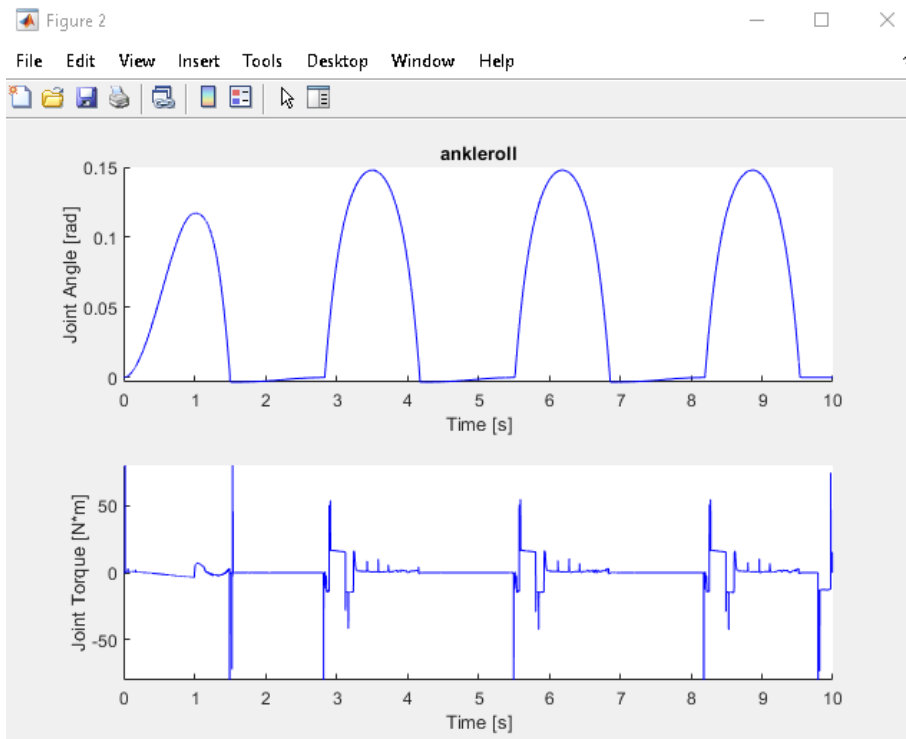


Fig 42: Ankle Roll

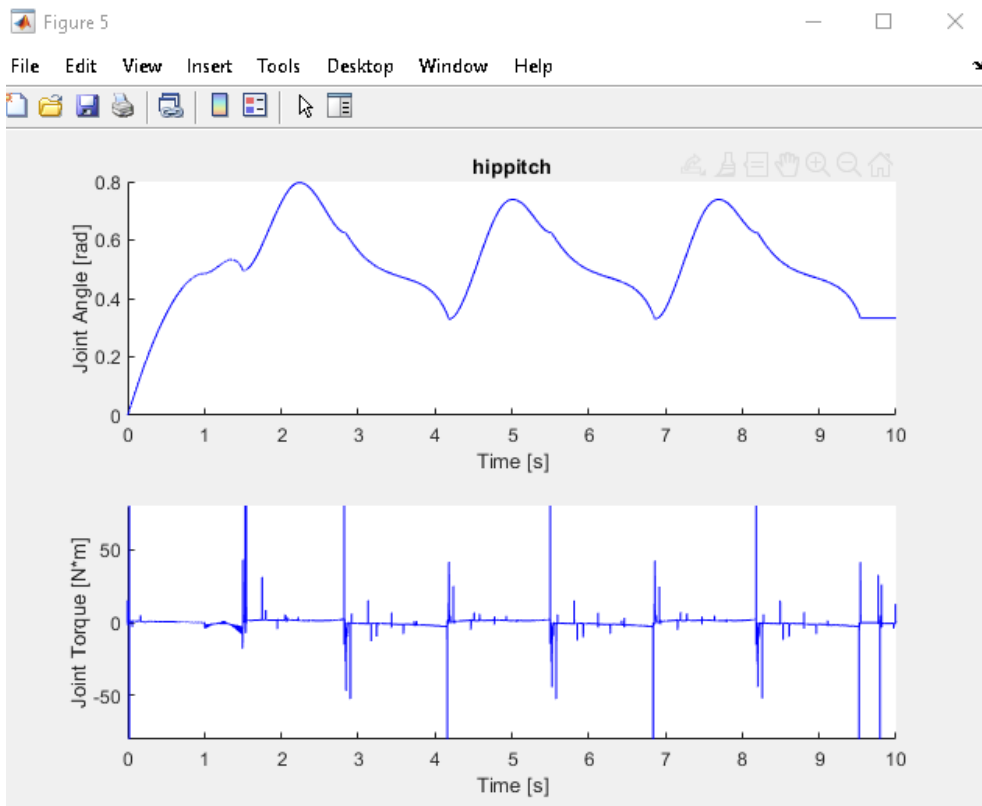


Fig 43: Hip Pitch

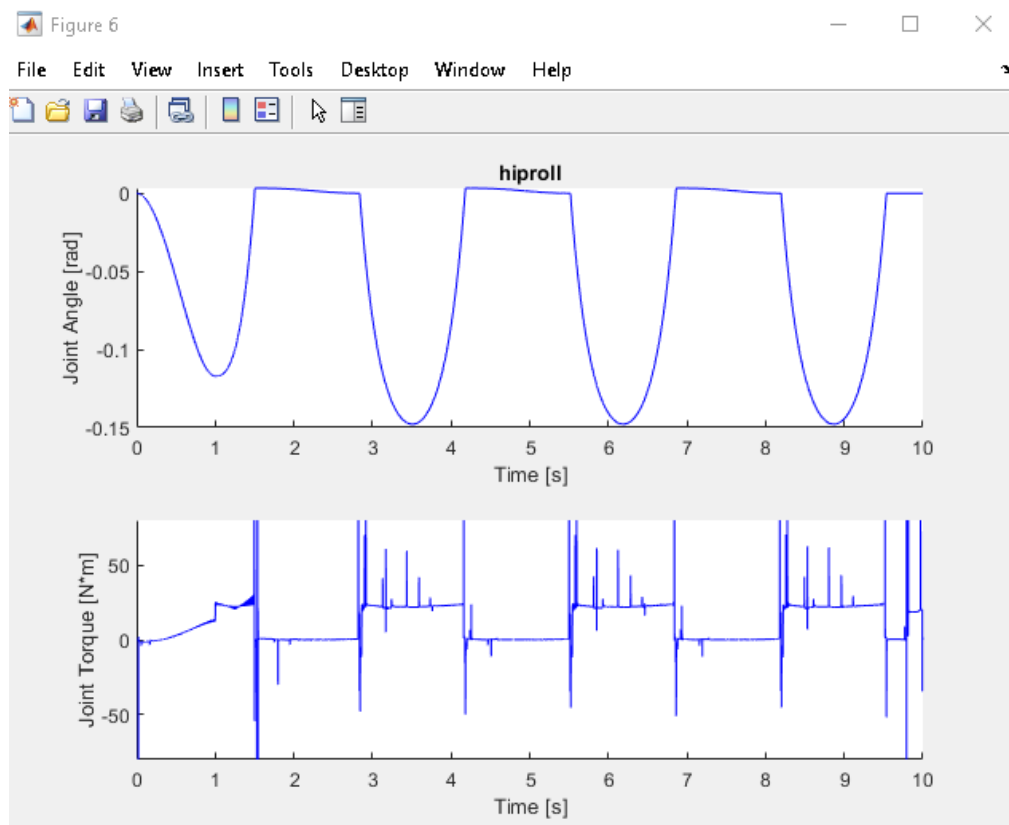


Fig 44: Hip Roll

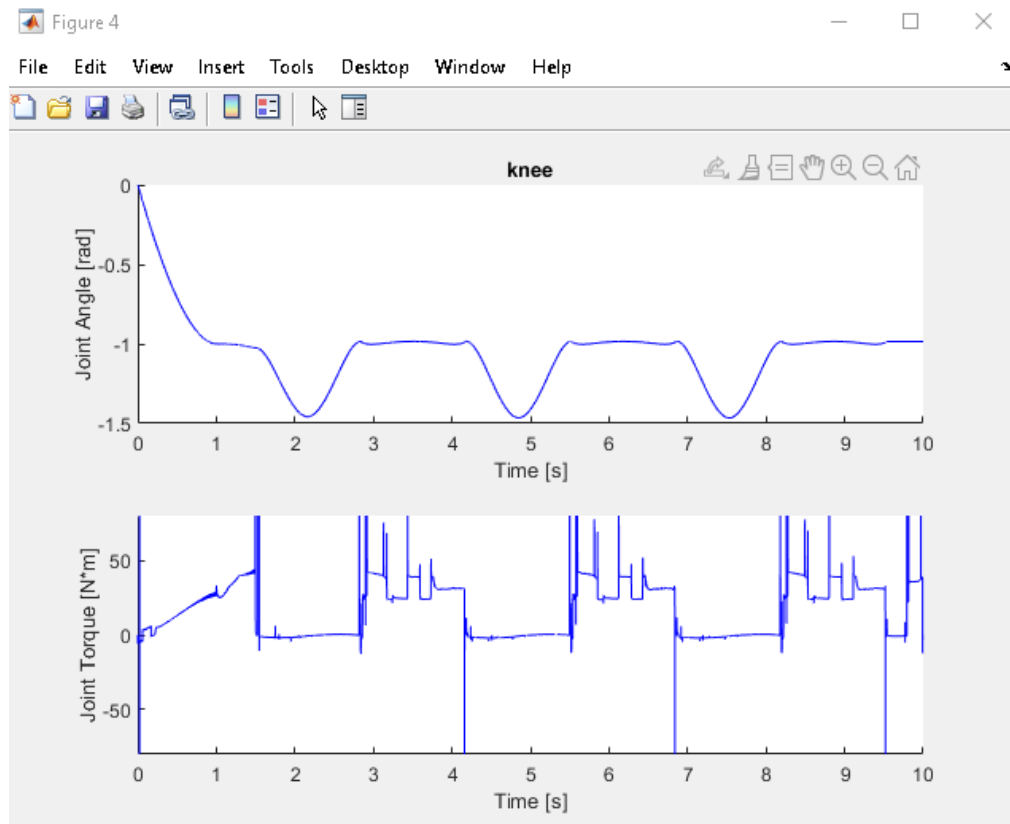


Fig 45: Knee

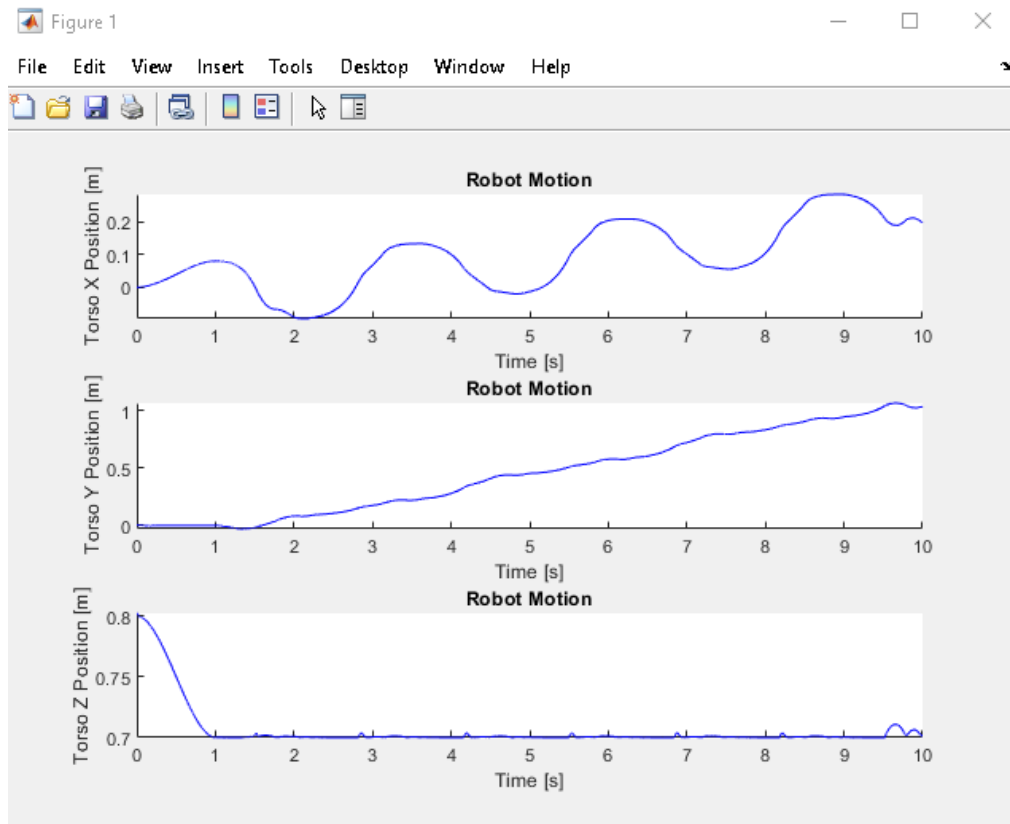


Fig 46: Robot Motion

11. CONCLUSION

Through the course of this project, I learned a great deal about strategies for designing and simulating walking robots. I will close my thesis report by summarizing my accomplishments and discussing the appropriate next steps in this project.

11.1 CONCLUSION BASED ON THEORY AND CALCULATIONS

Based on the calculations done, the robot is theoretically possible to build and will behave as per our initial conditions. The required torque will be made possible through adequate motors and the parameters for trajectory planning is fulfilled through formulations and theory.

11.2 CONCLUSION BASED ON SIMULATION AND ANALYSIS REPORT

Based on the report, some of the parts are to be optimized based on design requirements through using different approaches but most of them fulfill the required criteria.

11.3 EXTENSIONS OF WORK

The next logical step in this project was to test machine learning on the robot and to manufacture it in the future.

1. BIBLIOGRAPHY

- [1] Ill-Woo Park, Jung-Yup Kim, Jungho Lee and Jun - Ho Oh (2005), “Mechanical Design of Humanoid Robot Platform KHR-3 (KAIST Humanoid Robot - 3: HUBO)”, Proceedings of 2005 5th IEEE-RAS International Conference on Humanoid Robots
- [2] Ming Xie, Steven Dubowsky, Jean-guy Fontaine, Mohammad Osman Tokhi, Gurvinder S Virk, “Advances In Climbing And Walking Robots - Proceedings Of 10th International Conference (Clawar 2007)”, World Scientific, 2007
- [3] Jung-Yup Kim, Ill-Woo Park and Jun-Ho Oh (2004), “Design and Walking Control of the Humanoid Robot, KHR-2(KAIST Humanoid Robot - 2)”, ICCAS2004
- [4] Ivan Beker, “Proceedings of the XV International Scientific Conference on Industrial Systems (IS'11)”, FON, 2011
- [5] Aaron Edsinger-Gonzales and Jeff Weber,"A Force Sensing Humanoid Robot for Manipulation Research", "International Journal of Humanoid Robots"
- [6] Rodney A. Brooks, Cynthia Breazeal, Matthew Marjanovic, Brian Scassellati, Mathew M. Williamson,"Building a Humanoid Robot", "MIT Artificial Intelligence Lab"
- [7] SOPC DO : M: L HC Design and Implementation of Intelligent Control System for Autonomous Humanoid Robot based on SOPC Technology -. 9. 121 1. / . 121 2 0 2 . 2018/7/27 1 Control System Lab, Dept. of EE. , YZU
- [8] K. Hirai, M. Hirose, Y. Haikawa, and T. Takenaka, “The Development of Honda Humanoid Robot”, in Proc. IEEE Int. Conf. on Robotics and Automations, pp.1321-1326, 1998
- [9] J. Yamaguchi, A. Takanishi, and I. Kato, “Development of a biped walking robot compensating for three-axis moment by trunk motion”, in Proc. IEEE/RSJ Int. Conf. on Intelligent Robots and Systems, pp.561–566, 1993
- [10] Y. Sakagami, R. Watanabe, C. Aoyama, S. Matsunaga, N. Higaki, and K. Fujimura, “The intelligent ASIMO: System overview and integration”, in Proc. IEEE/RSJ Int. Conf. on Intelligent Robots and Systems, pp. 2478- 2483, 2002
- [11] K. Nishiwaki, T. Sugihara, S. Kagami, F. Kanehiro, M. Inaba, and H. Inoue, “Design and Development of Research Platform for PerceptionAction Integration in Humanoid Robot: H6”, in Proc. IEEE/RJS Int. Conf. on Intelligent Robots and Systems, pp.1559-1564, 2000
- [12] K. Kaneko, F. Kanehiro, S. Kajita, K. Yokoyama, K. Akachi, T. Kawasaki, S. Ota, and T. Isozumi, “Design of Prototype Humanoid Battery Main controller (PC) 325Robotics Platform for HRP”, in Proc. IEEE Int. Conf. on Intelligent Robots and Systems, pp.2431-2436, 1998

- [13] M. Gienger, K. Loffler, and F. Pfeiffer, “Towards the Design of Biped Jogging Robot”, in Proc. IEEE Int. Conf. on Robotics and Automation, pp.4140–4145, 2001
- [14] J. H. Kim, I. W. Park, and J. H. Oh, “Design of Lower Limbs for a Humanoid Biped Robot”, Int. Journal of Human friendly Welfare Robotic System, Vol.2, No.4, pp.5-10, 2002
- [15] J. H. Kim, S. W. Park, I. W. Park, and J. H. Oh, “Development of a Humanoid Biped Walking Robot Platform KHR-1 –Initial Design and Its Performance Evaluation–”, in Proc. of 3rd IARP Int. Work. on Humanoid and Human Friendly Robotics, pp.14–21, 2002
- [16] I. W. Park, Y. Y. Kim, S. W. Park, and J. H. Oh, “Development of Humanoid Robot Platform KHR-2(KAIST Humanoid Robot - 2)”, Int. Conf. on Humanoid 2004
- [17] J. Yamaguchi, and A. Takanishi, “Development of a Biped Walking Robot Having Antagonistic Driven Joints Using Nonlinear Spring Mechanism”, in Proc. of IEEE Int. Conf. in Robotics and Automation, pp.14–21, 1997
- [18] Jung-Yup Kim, Ill-Woo Park, Jungho Lee, Min-Su Kim, Baek-Kyu Cho and Jun-Ho Oh, “System Design And Dynamic Walking Of Humanoid Robot KHR-2”, IEEE International Conference on Robotics & Automation, 2005
- [19] J. J. Craig, Introduction to Robotics: Mechanics and Control, 2nd ed. (Addison-Wesley Publishing Company 1989), p.129
- [20] M. Gienger, K. Loffler and F. Pfeiffer, “Walking Control of a Biped Robot based on Inertial Measurement”, in Proc. of Int. Workshop. on Humanoid and Human Friendly Robotics, pp.22–30, 2002